Pergamon

Tetrahedron Vol. 50, No. 6, pp. 1777-1810, 1994

0040-4020/94 $6.00+0.00

0040-4020(93)E0087-V

Solution Conformation of Hexameric & Heptameric Lariat-RNAs and their Self-cleavage Reactions Which Give Products Mimicking Those From Some Catalytic RNAs (Ribozymes)

B. Rousse, N. Puri, G. Viswanadham, P. Agback, C. Glemarec, A. Sandström, C. Sund & J. Chattopadhyaya*

Department of Bioorganic Chemistry, Box 581, Biomedical Center, University of Uppsala, S-751 23 Uppsala, Sweden

Abstract: *The small "lariat" hexameric 1 and heptameric 2 RNAs undergo self-cleavage, whereas the two cyclic A(2'→5')G and A(3'→5')G linked tetramers 3 and 4 do not self-cleave. The site of phosphodiester cleavage is specific and occurs at the 3'-phosphate of the guanosine residue to give a guanosine 2',3'-cyclic phosphate and a 5'-hydroxyl termini. At 22 °C, the heptamer 2 ($k = 0.16 \times 10^{-3}$ min^{-1}) cleaves ca. six times faster than the hexamer 1 ($k = 0.25 \times 10^{-4}$ min^{-1}). The rate of cleavage is temperature and pH dependent. The addition of Mg^{2+} ions slightly increases the rate of cleavage, but NMR studies show that it does not produce any changes in the conformation of the ribose rings and of the glycosidic bonds. ^{1}H-NMR shows that the lariat-hexamer 1 exists as two conformers (A and B) in slow exchange on the NMR time scale. The enthalpy term ($\Delta H = 7.1$ kcal mol^{-1}) favours the A-form while the entropy term ($\Delta S = 21$ cal mol^{-1} K^{-1}) favours the B-form. The energy of activation for the transition between the A- and B-forms is 23 kcal.mol^{-1}. The loop nucleotides in the B-form of hexamer 1 have ribose, glycosidic bonds and phosphate backbone conformation that are very similar to those of heptamer 2. At low temperature, the conformation of the A(2'→5')G linked tetramer 3 and A(3'→5')G linked tetramer 4 is very similar to the conformation of the A-form of hexamer 1. Torsional constraints derived from ^{1}H-^{1}H, ^{1}H-^{31}P and ^{13}C-^{31}P coupling constants were used for molecular dynamics simulations in water with sodium counterions for a total of 226 ps. The MD simulations were first carried out with torsional constraints derived from J-couplings (0-96 ps) and then completely without constraints (106-226 ps). No major conformational changes occurred upon the release of the constraints indicating that the ensemble of conformers generated during the MD simulation are not artificially held in these conformations by the NMR constraints and these conformers may be good representatives of the actual NMR observed solution structures. A comparison of the self-cleavage rate between hexamer, heptamer and hammerhead-RNA ($k_{cat} \approx 0.5$ min^{-1} at 37 °C) also suggests that the cleavage-site geometry of the hammerhead-RNA should be much closer to the transition state/intermediate geometry than heptamer 2. The pH-dependent study of the self-cleavage reaction of hexamer 1 has shown that the self-cleavage rate peaks at pH 6 and slows down considerably both above and below this pH. Non-specific cleavage starts becoming important at a very low pH (≤3) and at a high pH (≥10). The structures generated during both NMR constrained and unconstrained MD runs show that the cleavage-site between G^3 and U^7 in heptamer 2 has the following average local conformation: S-sugar for G^3, ε^- (-86°±13°), ζ^+ (91°±16°), α^+ (85°±24°), β^t (163°±13°) and γ^+ (65°±11°). Molecular modelling studies on the MD generated geometry show that a simple rotation of the local phosphate backbone at the cleavage-site from ε^- ($d_{O2'\text{-}3'P} \approx 3.8$ Å) → $\varepsilon = 120°$ ($d_{O2'\text{-}3'P} = 2.8$ Å) and a rotation of $\zeta^+ \rightarrow \zeta^t$ would position the leaving 5'-terminus of U^7 for a potential in-line displacement by 2'-OH of G^3 (Note that in the latter geometrical transition, α^+, β^t and γ^+ and the South-sugar of U^7 remain unchanged). Such a geometry at the cleavage site would produce an optimal local structure for a neighbouring nucleophilic attack by 2'-OH to give the trigonal-bipyramidal phosphorane transition state/intermediate.*

The catalytic activity of some RNA domains includes the site specific self-cleavage of a phosphodiester bond to give a 5'-hydroxyl and a 2',3'-cyclic phosphate termini[1]. Four different domains of this type have been identified so far: (i) The hammerhead ribozyme[1], (ii) The hairpin ribozyme[2], (iii) Delta ribozyme[3] and (iv)

Neurospora mitochondrial domain[4]. The self-cleavage occurs by a transesterification reaction which takes place by the direct attack of the 2'-oxygen on the phosphate and by in-line displacement of the 5'-oxygen. The reaction probably occurs via a trigonal bipyramidal phosphate that may be a transition state or an intermediate[5]. The self-cleavage reaction in the systems above requires the presence of divalent metal ions. Biological, biochemical and kinetics data on the hammerhead and hairpin ribozyme have suggested that specific functional groups of the conserved nucleotide residues are critical for the formation of the self-cleavage complex[6]. Very few structural information are however available except four NMR studies[7] involving exchangeable imino protons which have confirmed the presence of three helical regions in the hammerhead domain. To understand the mechanism of self-cleavage reaction and the local conformation necessary for the self-cleavage at a particular phosphodiester bond, it will however be necessary to determine their three dimensional structure. These structural studies are difficult with natural self-cleaving hammerhead type systems, if not impossible, because the catalytically active natural RNA molecule are large, forming complicated tertiary structures, and have a rate of self-cleavage which is far too quick at an ambient temperature ($k \approx 0.5\ min^{-1}$) to be amenable to conformational studies by NMR spectroscopy. Recently, it has been shown that selective and complete hydrolysis can occur also on molecules as small as tetramers in the presence of a cofactor[8]. The oligoribonucleotide sequence as well as hydrogen bond interactions are important for the selectivity of hydrolysis[8].

In this paper, we present our detailed NMR studies on the solution conformation of two small model lariat RNAs, a hexamer **1** and a heptamer **2**, which mimick the sequence at and around the branch-point in Group II type splicing and undergo site-specific self-cleavage to give **5** and **6**, respecively[9]. The product (*i.e.* **5** and **6**) of the self-cleavage reaction of **1**→ **5** and **2** → **6** is also a 2',3'-cyclic phosphate and a 5'-hydroxyl termini, but the reaction does not require any divalent metal ions or cofactors. The hexamer **1** and heptamer **2** are to our knowledge the first examples of RNAs which undergo site-specific self-cleavage in the absence of ribonuclease, divalent metal ions or any other cofactor. The conformation of two cyclic tetramers, **3** and **4**, which have the same loop nucleotides as hexamer **1** but no 2'- or 3'-tail attached to the adenosine branch-point and do not self-cleave is also reported. The results from the kinetics and conformational analysis have provided information on the conformational and functional requirements for the self-cleavage of **1** and **2**. The data indicates that conformational flexibility of the nucleotides in the loop, as well as interactions with some specific function, presumably the 4-amino group or the N^3 of cytosine, of the 3'-tail is necessary for the self-cleavage reaction.

Chemistry

The cyclic (2'→5') linked tetramer **3** was prepared (Scheme 1) according to the procedures developed in the phosphotriester chemistry[10]. The 5'-hydroxy-adenosine block **11**, which was synthesized according to our published procedure[11-14], was condensed with the 3'-phosphodiester block **10b** *using* 1-*mesitylene*-sulfonyl-3-nitro-(1,2,4-triazole) (MSNT) as the condensing agent to give the trimer **12a** (77%). Treatment of **12a** with trichloroacetic acid[15] in a solution of $MeOH/CH_2Cl_2$ (2:98, v/v) gave the corresponding 5'-hydroxy block **12b** (66%). Compound **12b** and the 3'-phosphodiester block **13** were condensed using MSNT to afford the tetramer **14a** (84%), which was detritylated using similar condition as described for **12a** to give **14b** (84%). Finally, the 5'-hydroxy-tetramer **14b** was treated with a solution of triethylamine (20 equiv) in dry

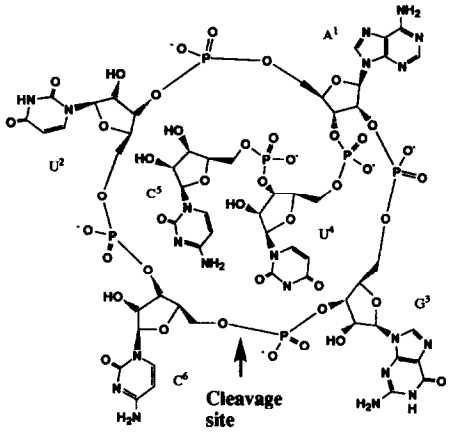

1

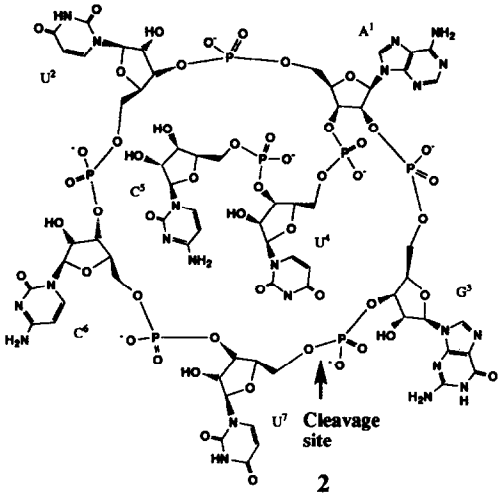

2

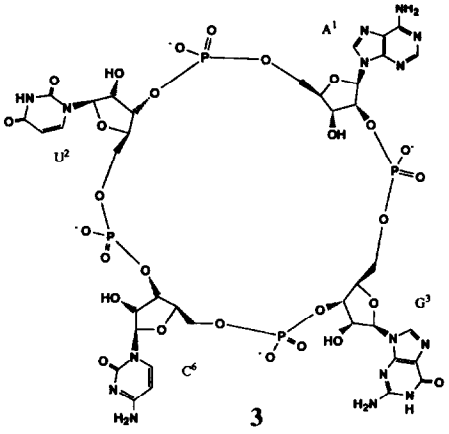

3

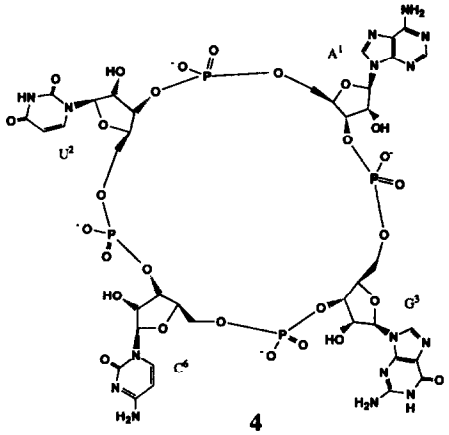

4

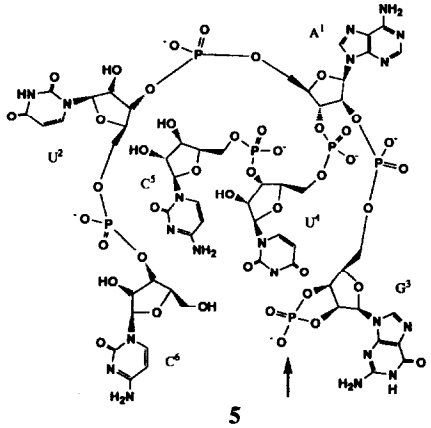

5

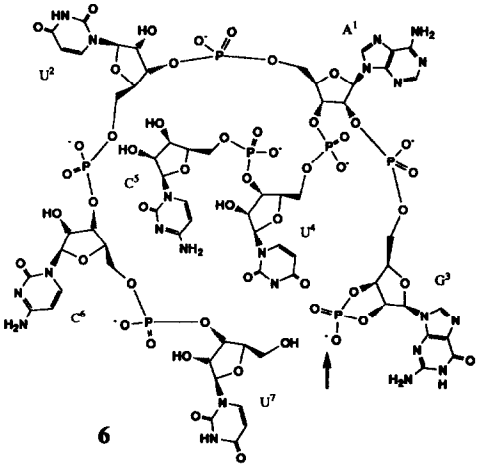

6

pyridine (0.2 M) to give the key phosphodiester block **14c** (98%). The intramolecular cyclisation of **14c** was achieved in dry pyridine solution (4 mM) in presence of MSNT (24 equiv.) to give the fully protected cyclic (2'→5')-linked tetramer **15** (33%). Deprotection of **15** in 4 steps in the usual manner[16] gave **3** (24%).

The cyclic (3'→5')-linked tetramer **4** was prepared (Scheme 1) by the condensation of **16** and **10c** using MSNT as the condensing agent to give the fully protected tetramer **17a** (81%). The 5'-O-Dmtr group was then removed from **17a** by treatment with trichloroacetic acid in a MeOH-CH_2Cl_2 solution (2:98,v/v) at 0 °C to give **17b** (78%). **17b** was treated with a solution of triethylamine (20 equiv.) in dry pyridine (0.2 M) to afford the phosphodiester block **17c** (71%). The intramolecular cyclisation of **17c** was carried out in dry pyridine under high dilution (250 ml / mmol, 4 mM) in presence of MSNT to give the fully protected cyclic tetramer **18** (85%). **18** was deprotected in 3 steps according to the published procedures[16] to give tetramer **4** (31%).
The hexamer **1** was prepared essentially using our published procedure[16] with minor modifications (Scheme 1). The dimer **10a** was condensed with N6-benzoyl-2'-O-(9-phenylxanthen-9-yl (Pixyl))adenosine **19** in regioselective manner to give the trimer **20a** (66%), which was converted to 3'-(2-chlorophenyl)phosphate **20b** (94%). The 2'-O-pixyl group was then removed from **20b** to give **20c** (77%), which was then phosphorylated using bis(cyanoethyl)phosphoroamidite[17], followed by an oxidation step to give the branch-point 2',3'-vicinal phosphate derivative **20d** (50%) using the procedures developed in phosphoramidite chemistry[18]. The chain extension at the 3'-end of **20d** was then carried out by a condensation reaction with dimer **21** in pyridine solution in presence of (MSNT) to give the pentamer **22a** (54%). The 5'-levulinyl group was then removed from **22a** by a brief treatment of hydrazine hydrate in pyridine-acetic acid solution (3:2, v/v) to give **22b** (73%). A chain extension at the 5'-end of **22b** was then carried out by a condensation with the guanosine nucleotide block **23** in pyridine solution in presence of MSNT to give hexamer **24a** (90%). The 5'-levulinyl group was then removed from **24a** by a brief treatment of hydrazine hydrate in pyridine-acetic acid solution (3:2, v/v) to give **24b** (66%). The 2'-bis(cyanoethyl)phosphate function at the branch-point adenosine was then converted to the corresponding 2'-phosphodiester function by brief treatment with diisopropylethylamine in pyridine solution to give **24c** (67%). The oligomer **24c** was intramolecularly cyclized to give protected hexameric lariat RNA **25** (72%) using MSNT (9 equiv.) as the activating agent in pyridine solution (250 ml / mmol of **24c**). The protected hexameric lariat RNA **25** was subsequently deprotected in the usual manner[16] to give the hexameric lariat RNA **1** (28%). The hexamer **1**, tetramers **3** and **4** have been characterised by 1D and 2D NMR. The synthesis of heptamer **2** has been previously reported from this laboratory[19].

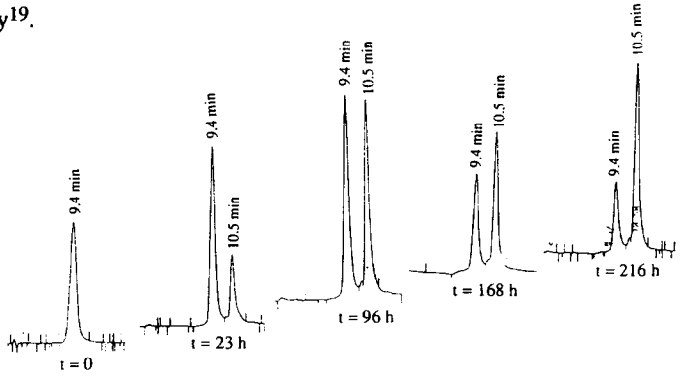

Figure 2: The Hplc elution profiles at different time intervals of the self-cleavage reaction of lariat hexamer **1** at 22°C in presence of Mg^{2+} ions to give the self-cleaved hexamer **5** (See experimental for conditions). The hexamer **1** eluted at R_t = 9.40 min and the self-cleaved hexamer **5** eluted at R_t = 10.50 min.

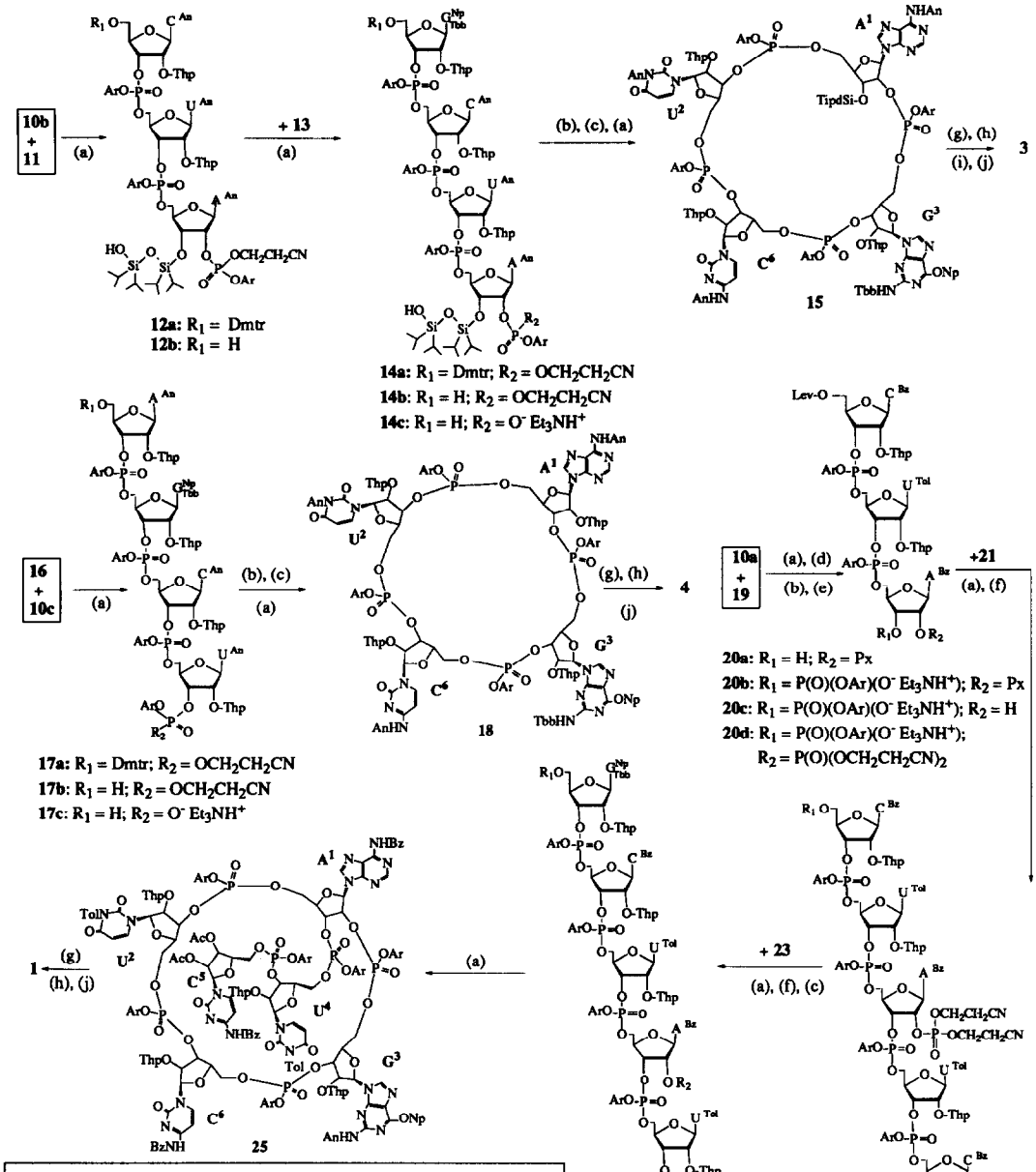
10b + 11
(a)
+ 13
(a)
(b), (c), (a)
(g), (h)
(i), (j)
3
12a: R1 = Dmtr
12b: R1 = H
14a: R1 = Dmtr; R2 = OCH2CH2CN
14b: R1 = H; R2 = OCH2CH2CN
14c: R1 = H; R2 = O- Et3NH+
15
16 + 10c
(a)
(b), (c)
(a)
(g), (h)
(j)
4
17a: R1 = Dmtr; R2 = OCH2CH2CN
17b: R1 = H; R2 = OCH2CH2CN
17c: R1 = H; R2 = O- Et3NH+
18
10a + 19
(a), (d)
(b), (c)
+21
(a), (f)
20a: R1 = H; R2 = Px
20b: R1 = P(O)(OAr)(O- Et3NH+); R2 = Px
20c: R1 = P(O)(OAr)(O- Et3NH+); R2 = H
20d: R1 = P(O)(OAr)(O- Et3NH+);
R2 = P(O)(OCH2CH2CN)2
(g)
(h), (j)
1
(a)
+ 23
(a), (f), (c)
22a: R1 = Lev
22b: R1 = H
24a: R1 = Lev; R2 = P(O)(OCH2CH2CN)2
24b: R1 = H; R2 = P(O)(OCH2CH2CN)2
24c: R1 = H;
R2 = P(O)(OCH2CH2CN)(O- (i-Pr)2NH+)
25
REAGENTS
(a): N-methylimidazole, Ms-Cl, pyridine, or MSNT , pyridine at RT;
(b) : TCA , 2% MeOH-CH2Cl2, 0 °C; (c) : (i-Pr)2EtN (30 eq), pyridine, 40 °C;
(d) : O-chlorophenylphosphoro-bis-(1,2,4 triazolide), pyridine, MeCN at RT;
(e): (Ce O)2P N(i-Pr)2 /tetrazole, MeCN/DMF at RT;
(f): Hydrazine hydrate, pyridine/AcOH (3:2) at RT;
(g): TMG /NBO , dioxane/H2O (8;2) at RT; (h): Conc. NH3 (aq) at RT;
(i): TBAF .3H2O, THF at RT; (j): 80% aq. AcOH at RT.

Scheme 1

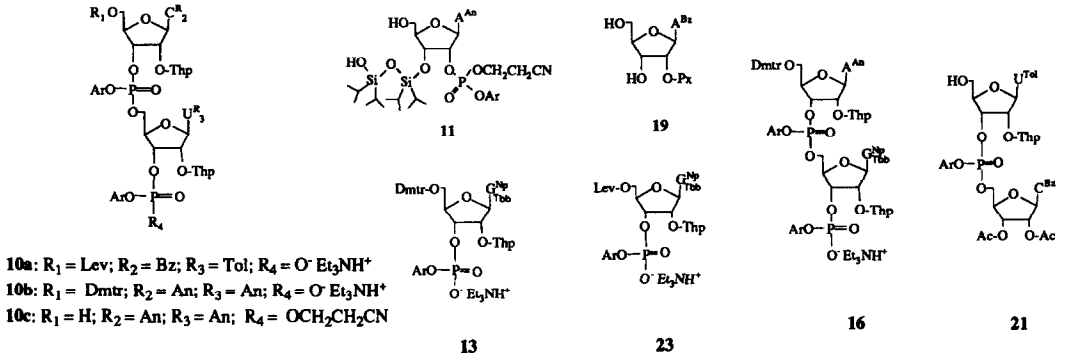

10a: R_1 = Lev; R_2 = Bz; R_3 = Tol; R_4 = O^- Et_3NH^+
10b: R_1 = Dmtr; R_2 = An; R_3 = An; R_4 = O^- Et_3NH^+
10c: R_1 = H; R_2 = An; R_3 = An; R_4 = OCH_2CH_2CN

11 **19** **13** **23** **16** **21**

Abbreviations
A = adenine-9-yl; AcOH = acetic acid; An = 4-anisoyl or 4-methoxybenzoyl; Ar = 2-chlorophenyl; Bz = benzoyl; C = cytosine-1-yl; Ce = 2-cyanoethyl; DMF = dimethylformamide; Dmtr = 4,4'-dimethoxytrityl; G = guanine-9-yl Lev = levulinyl; Ms-Cl =1-mesitylenesulfonyl chloride; MSNT = 1-mesitylenesulfonyl-3-nitro-1,2,4-triazole; NBO = *syn*-4-nitrobenzaldoxime; Np = 2-nitrophenyl; Px = pixyl or 9-phenylxanthen-9-yl; TBB = 4-(t-butylbenzoyl); TBAF = tetrabutylammonium fluoride; Thp = tetrahydropyran-2-yl; TMG = 1,1,3,3-tetramethylguanidine; Tol = 4-toluoyl; U = uracil-1-yl.

Scheme 1 (contd.)

Self-cleavage reaction of lariat RNA

The hexamer **1** and heptamer **2** undergo site specific self-cleavage whereas the cyclic A(2'→5')G linked tetramer **3** and the cyclic A(3'→5')G linked tetramer **4** do not self-cleave. The product of the self-cleavage reaction of **1** and **2** has been characterised by NMR and by Hplc, and the cleavage reaction has been studied under a variety of different reaction conditions (temperature, concentration, pH, presence of Mg^{2+} ions).

(a) Characterisation of the self-cleaved product: At 22°C, the ^1H- and ^{31}P-NMR spectrum of **1** and **2** showed the appearence of another set of resonances (**1**→ **5** and **2** → **6**) whose intensities increased as a function of time while the intensities of **1** and **2** decreased proportionally. One of the ^{31}P-NMR resonances of **5** and **6** is very deshielded (21.4 ppm) compared to all other phosphates, and has a chemical shift which is characteristic for a 2', 3'-cyclic phosphate[20]. All the ^1H and ^{31}P resonances of **5** and **6** were assigned by means of several 2D-NMR experiments such as clean-TOCSY, COSY, NOESY and ^1H-^{31}P chemical shift correlation experiments (Tables 2 and 3, Fig. 1). The ^1H-^{31}P chemical shift correlation spectra connect the H2' and H3' of the G^3 residue in **5** and **6** with its cyclic phosphate residue at 21.4 ppm with $^3J_{H2',P2'} = {}^3J_{H3',P2'}$ = 8.1 Hz (Fig. 1). This phosphate at 21.4 ppm does not show any correlation with 5'/5" protons. All the other phosphodiesters of **5** and **6** absorb between 0.25 and 0.90 ppm and they all showed connectivities to both a 3'- and to 5'/5" protons (Fig. 1, Table 3), which evidenced that no other unspecific phosphodiester cleavage has taken place in the lariat-RNAs. The specificity of the self-cleavage reaction is also clearly established from the fact that almost all expected proton-phosphorous couplings have been found through the subtraction of phosphorous-coupled and -decoupled DQF-COSY spectra (see Table 5). From these experiments, it could be concluded beyond any doubt that the specific site of the phosphodiester cleavage in **1** and **2** occurs at the 3'-phosphate of the G^3 residue to give 2', 3'-cyclic phosphate G^3 and a 5'-hydroxyl terminal nucleotide in **5**

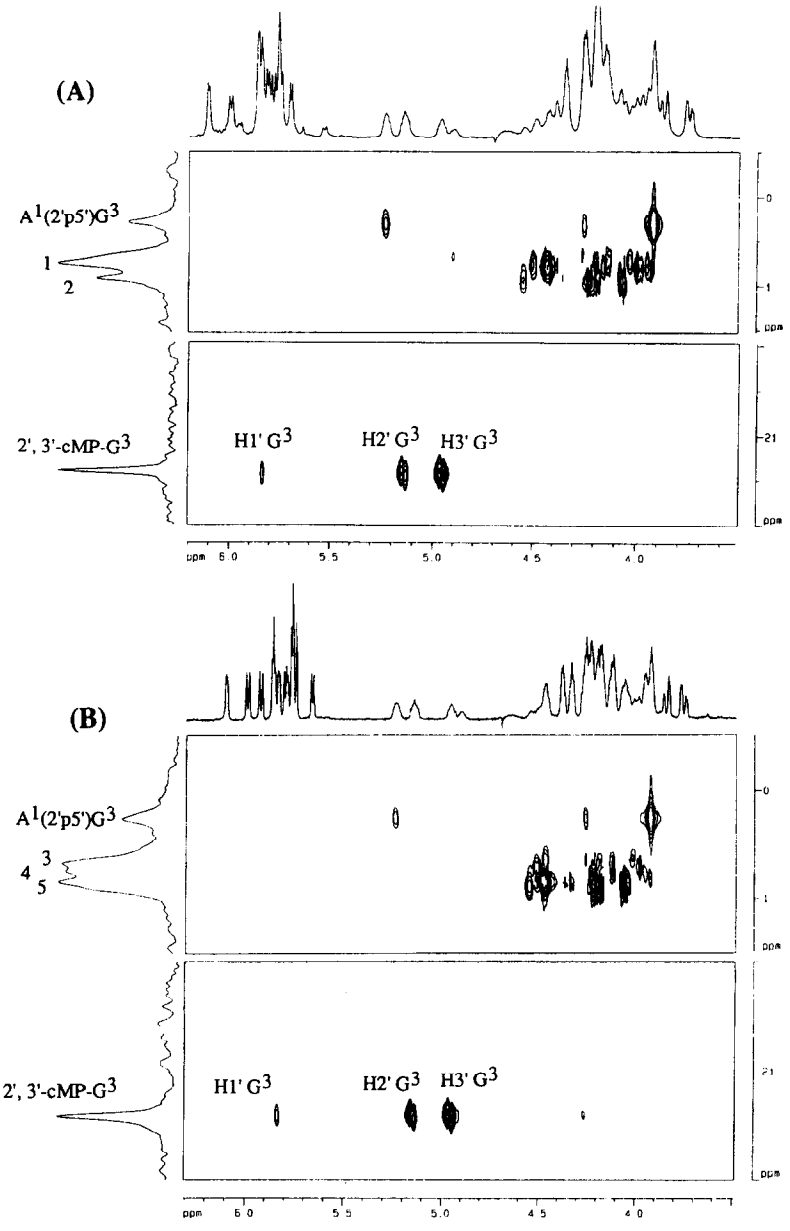

Figure 1: ^{1}H-^{31}P chemical shift correlation spectra of the self-cleaved hexamer **5** (panel A) and the self-cleaved heptamer **6** (panel B) at 298K in $^{2}H_2O$. In both cleaved RNAs, the 2', 3'-cyclic phosphate of G^3 absorbs at 21.4 ppm and shows strong cross peaks with the H2' and H3' as well as a weak cross peak with the H1'. The spectrum was cut along the ^{31}P axis between 1.5 and 22 ppm to be able to see the 3' and 5' phosphates which all absorb between 0.5 and 1 ppm. (1) A^1(3'p5')U^4, U^2(3'p5')A^1, C^6(3'p5')U^2, (2) U^4(3'p5')C^5, (3) A^1(3'p5')U^4, U^7(3'p5')C^6, (4) C^6(3'p5')U^2, (5) U^2(3'p5')A^1, U^4(3'p5')C^5.

and **6** (5'-OH of C^6 in **5** and 5'-OH of U^7 in **6**). The simultaneous Hplc (Fig. 2) and NMR study monitoring the progress of the self-cleavage reaction of hexamer **1** for 64 days at 22 °C showed only the formation of *one cleavage product* which is the 2',3'-cyclic phosphate **5**, ruling out any ribonuclease promoted cleavage. Any ribonuclease promoted cleavage is also ruled out by the fact that circular RNAs such as **3** and **4** and tetrameric[9] and pentameric[9] lariat RNAs are completely stable.

(b) Concentration dependence:

The rate of the cleavage reaction of hexamer **1** has been determined at 22°C, pH 6.7 at three different concentrations, and shows virtually no dependence on concentration. The cleavage reaction was followed by NMR spectroscopy for the high concentrations (2 and 4 mM, $k = 0.25.10^{-4}$ min^{-1}) and by Hplc for the low concentration (0.17 mM, $k = 0.40\ 10^{-4}$ min^{-1}). The cleavage reaction of heptamer **2** was followed by NMR at 22°C for a sample concentration of 4 mM. At 22°C, the heptamer **2** cleaves ($k = 0.16\ 10^{-3}$ min^{-1}) *ca.* six times faster than the hexamer **1** ($k = 0.25\ 10^{-4}$ min^{-1}). We found that the triethylammonium salt of **1** and **2** did not self-cleave, which suggests that the bulky triethylammonium ion could exert some steric hindrance which inhibits or reduces the ability to form the intermediate or transition state required for cleavage.

(c) pH dependence:

The pH dependence of the cleavage reaction at 35°C for hexamer **1** was followed by Hplc, for a concentration of 0.17 mM. The data on the half-lives of the self-cleavage reactions for hexamer **1** (Table 1) shows that a maximum rate enhancement of the self-cleavage reaction takes place at pH 6 with the rates decreasing on both above and below this pH. The rate acceleration of the self-cleavage reaction found at a very low pH (≤3) is presumably due to general intermolecular acid catalysis which takes place due to the protonation of the phosphodiester oxygen. On the other hand, the rate acceleration found at a high pH (≥10) is presumably due to general intermolecular base catalysis which takes place due to the formation of the conjugate anion of the 2'-hydroxy function, which, in turn, participates in the nucleophilic attack in a facile manner to the vicinal phosphate. The Hplc analysis of the self-cleavage reaction at pH ≤3 and ≥10 have revealed the formation of other products besides the specific self-cleavage product **5**, which means that other non-specific acid-catalyzed or base-catalyzed cleavage reactions are as well occurring under these extreme reaction conditions. The fact that the sef-cleavage rate peaks at pH 6 (Table 1) suggests that all the constituent phosphodiester functions (pK_a ~1.5) should be in the ionic form and the vicinal 2'-hydroxyl (pK_a ~13) in the non-ionized form. *This means that most probably an intramolecular acid-base catalysis is an important event that takes place optimally at pH 6 in which phosphate acts as an internal base catalyst to abstract the proton from the vicinal 2'-OH. The question then becomes, why does the specific phosphodiester bond between G^3 and C^6/U^7 undergo self-cleavage through transesterification reaction in a regiospecific manner? The answer to this key question is most probably that the sugar-phosphate backbone torsions of this specific phosphodiester can energetically in a preferential manner access a certain hyperspace of conformations that are prerequisite to form the transient trigonal bipyramidal phosphorane which cleaves to 2',3'-cyclic phosphate and 5'-hydroxyl termini.* The fact that the rate of self-cleavage is not concentration-dependent rules out any involvement of intermolecular catalysis.

(d) Effect of Mg^{2+} ions:

The addition of magnesium ions (2 equiv, pH 6.7, 22 °C) increases the rate of cleavage of hexamer **1** (Table 1). The riboses and the glycosidic bond conformation of the constituent nucleotides of **1** did not

however change upon addition of Mg^{2+} ions suggesting that most probably Mg^{2+} ion binds to the exocyclic phosphate-oxygen (*vide infra*).

Table 1: The pH dependence of the self-cleavage reaction of hexamer **1**.

pH*	$t_{1/2}$ (h)	$t_{1/2}$ (h) with 2 eq. Mg^{2+}
2.0	64	/
3.0	311	288
4.0	617	455
5.0	294	275
6.0	185	140
7.1	315	222
8.0	420	287
9.0	538	355
10.0	215	178
11.0	82	20
12.0	7	4

*Buffer: 0.2 M KCl-0.2 M HCl (pH 2); 0.1 M citric acid-0.2 M Na_2HPO_4 (pH 3-6); 0.1 M Tris-0.1 M HCl (pH 7 -9); 0.1 M Na_2CO_3 - 0.1 M $NaHCO_3$ (pH 10); 0.05 M $NaHCO_3$- 0.1 M NaOH (pH 11); 0.2 M KCl- 0.2 M NaOH (pH 12). T = 308 K, hexamer concentration = 0.17 mM, magnesium ions concentration = 2 equivalents.

(e) Temperature dependence:

The rate of cleavage of hexamer **1** (0.17 M) was measured at a number of different temperatures (22°C, 25°C, 28°C, 35°C, 45°C, 50°C and 55°C) by Hplc at pH 6.8 buffer (see the footnote of Table 7). The rate is temperature dependent and reaches a maximum at ~45°C. Above 45°C, the rate of the reaction decreases suggesting that the conformation necessary for the self-cleavage is not able to form at a higher temperature. The Arrhenius plot ln(k) vs. 1/T is linear between 22 and 35°C and gives an energy of activation E_a of ~52 kcal.mol^{-1}. In the presence of magnesium ions, the energy of activation of the cleavage reaction is lowered to ~17 kcal.mol^{-1}.

The cyclic A(2'→5')G linked tetramer **3** and the cyclic A(3'→5')G linked tetramer **4** at a concentration of 4 mM were kept at room temperature for 30 days. During this time, no trace of self-cleavage or normal RNA degradation were observed. We have not yet been able to find an appropriate system for HPLC or capillary electrophoresis or simple polyacrylamide gel electrophoresis for the separation of heptamer **2** from its cleavage product **6**.

Conformational study by NMR (^{1}H at 500 MHz)

(a) Assignment:

The proton and phosphorus resonances of **1-6** have been assigned using 2D experiments, such as clean-TOCSY[21], NOESY[22], ROESY[23], DQF-COSY[24] and ^{1}H-^{31}P chemical shift correlation[25] experiments.The J-coupling network for each sugar residue was identified from clean-TOCSY and DQF-COSY. NOESY or ROESY were used to connect the aromatic protons of the nucleobases to their sugar units. The ^{1}H-NMR and ^{31}P-NMR chemical shifts for **1-6** are given in Tables 2 and 3. The hexamer **1** shows two sets of proton resonances (Figures 3 and 4) which can be attributed to two conformers (A- and B-form) in slow exchange on the NMR time scale (*vide infra*). At low temperature, the A-form is predominant (90 %

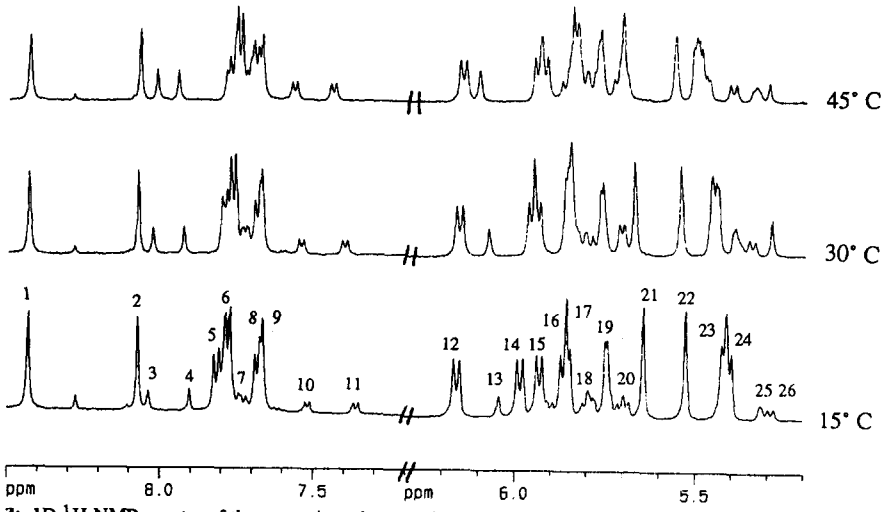

Figure 3: 1D ^{1}H-NMR spectra of the aromatic and anomeric region of the interconverting A- and B-form of lariat hexamer **1**. Upon an increase of temperature, the intensity of the resonances corresponding to the B-form become more intense. (1) H8 A^1, A-form; (2) $H2A^1$, A-form, (3) $H8A^1$, B-form; (4) $H2A^1$, B-form; (5) $H6U^4$, A-form; (6) $H6U^2$ & C^5, A-form; (7) $H6U^2$ & C^5, B-form; (8) $H6C^6$ A-form; (9) $H8G^3$, A-form; (10) $H6C^6$, B-form; (11) H6 U^4, B-form; (12) $H1'A^1$, A-form; (13) $H1'A^1$, B-form; (14) $H1'U^2$, A-form; (15) $H5C^5$, A-form; (16) H1' U^2, B-form, $H5U^4$, A-form; (17) $H1'U^4$ A-form; (18) $H5U^2$, C^5, C^6, B-form; (19) $H1'C^5$, A-form, $H1'C^5$, B-form; (20) $H1'G^3$ & C^6, B-form; (21) $H1'C^6$, A-form; (22) $H1'G^3$, A-form; (23) $H5C^6$, A-form; (24) H5 U^2, A-form; (25) $H5U^4$, B-form; (26) $H2'A^1$, B-form. † signifies impurity.

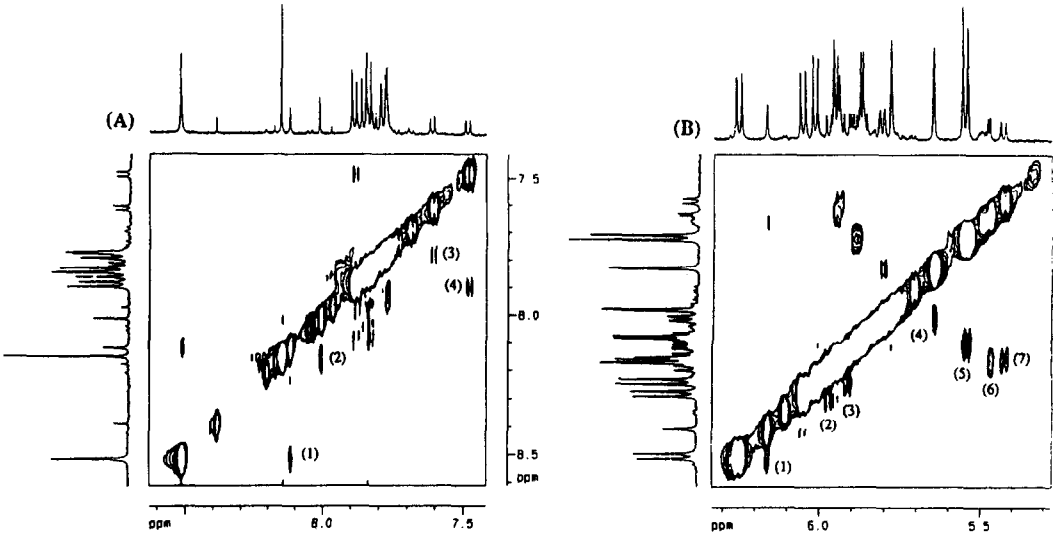

Figure 4: 2D NOESY / chemical exchange spectra of hexamer **1** at 303K in ^2H_2O. Panel A shows cross peaks resulting from chemical exchange between the A- and B-forms in the aromatic region with (1): $H8A^1$, (2): $H2A^1$, (3): $H6C^6$, (4): $H6U^4$. Panel B shows chemical exchange cross peaks for the H1' and H5 region with (1): $H1'A^1$, (2): $H1'U^2$, (3): $H5C^5$, (4): H1' G^3, (5): $H5U^2$, $H5C^6$, (6): $H1'U^4$, (7): $H5U^4$. This experiment has been used to assign some of the resonances of the B-form from the corresponding A-form assignment.

Table 2: ^{1}H- and ^{31}P-NMR chemical shifts (ppm, ^{1}H referenced to CH_3CN set at 2.00 ppm, ^{31}P referenced to cAMP set at 0.00 ppm) of **1** - **4** in $^{2}H_2O$. T = 298 K for **1**, **3**, **4** , and T = 284 K for **2**).

		A^1	U^2	G^3	U^4	C^5	C^6	U^7
Hexamer **1** A-form	H1'	6.26	6.08	5.64	5.96	5.86	5.76	
	H2'	5.13	3.96	4.57	4.44	4.27	4.19	
	H3'	4.81	4.77	4.76	4.61	4.21	4.37	
	H4'	4.60	4.37	4.35	4.46	4.25	4.37	
	H5'	4.41	4.10	4.28	4.28	4.16	4.11	
	H5"	4.27	4.10	4.08	4.18	4.12	4.08	
	H8	8.55	-	7.77	-	-	-	
	H2	8.21	-	-	-	-	-	
	H6	-	7.89	-	7.91	7.90	7.80	
	H5	-	5.54	-	5.97	6.07	5.55	
Hexamer **1** B-form	H1'	6.18	5.98	5.81	5.48	5.85	5.81	
	H2'	5.50	4.36	5.00	4.18	4.15	4.19	
	H3'	4.57	4.54	4.82	4.41	4.23	4.37	
	H4'	4.53	4.53	4.47	4.33	4.15	4.29	
	H5'	4.38	4.25	4.25	4.06	4.03	4.09	
	H5"	4.35	4.21	4.25	4.03	4.03	4.09	
	H8	8.15	-	7.90	-	-	-	
	H2	8.04	-	-	-	-	-	
	H6	-	7.84	-	7.51	7.86	7.67	
	H5	-	5.90	-	5.45	5.94	5.93	
Heptamer **2**	H1'	6.09	5.62	5.67	5.78	5.86	5.95	5.99
	H2'	5.29	4.16	4.84	4.33	4.18	4.35	4.39
	H3'	5.04	4.50	4.69	4.54	4.26	4.62	4.64
	H4'	4.41	4.12	4.44	4.41	4.20	4.38	4.48
	H5'	4.25	3.89	4.14	4.29	4.08	4.22	4.39
	H5"	3.90	3.86	3.96	4.14	4.06	4.15	4.18
	H8	8.11	-	7.78	-	-	-	-
	H2	7.93	-	-	-	-	-	-
	H6	-	7.63	-	7.76	7.81	7.81	7.86
	H5	-	5.79	-	5.77	5.99	5.99	5.88
	2'P	0.05						
	3'P	0.40	0.34	0.90	0.77		0.69	0.90
Tetramer **3**	H1'	6.27	5.97	5.71			5.71	
	H2'	5.13	4.05	4.82			4.29	
	H3'	4.73	4.56	4.70			4.70	
	H4'	4.29	4.39	4.45			4.31	
	H5'	4.13	4.16	4.29			4.40	
	H5"	4.07	4.10	4.17			4.34	
	H8	8.43	-	7.83			-	
	H2	8.15	-	-			-	
	H6	-	7.90	-			7.67	
	H5	-	5.67	--			5.33	
	3'P	0.01(2'P)	1.13	0.19			0.89	
Tetramer **4**	H1'	6.12	5.94	5.82			5.81	
	H2'	4.89	4.15	4.71			4.23	
	H3'	4.88	4.68	4.79			4.46	
	H4'	4.56	4.34	4.49			4.33	
	H5'	4.27	4.13	4.21			4.30	
	H5"	4.07	4.07	4.10			4.30	
	H8	8.51	-	7.96			-	
	H2	8.18	-	-			-	
	H6	-	7.82	-			7.71	
	H5	-	5.55	-			5.54	
	3'P	0.51	1.25	0.34			0.98	

A-form at 5°C), but as the temperature is raised (5°C to 45°C), the resonances attributed to the B-form become more intense (57 % A-form at 45°C), while those assigned to the A-form decrease in intensity (Figure 3). The population of A- *versus* B-form is independent of concentration and on the nature of counter cation (Na^+ or Et_3NH^+ ion). The observation of chemical exchange connectivities in the NOESY spectrum (Figure 4), as well as saturation transfer experiments between the two sets of resonances (*vide infra*), have confirmed that the A- and B-forms are two interconverting conformers in slow equilibrium on the NMR time scale.

The conformational properties of **1-6** have been investigated using vicinal $^3J_{HH}$, $^3J_{HP}$ and $^3J_{CP}$ coupling constants (Tables 4 and 5). Intraresidual nOes were used to determine the conformation of the glycosidic bond. No interresidual nOe cross peaks were observed in the NOESY spectra. The correlation time τ_c was found to be 0.5 ± 0.3 ns for **1** and 0.7 ± 0.3 ns for **2** giving $\omega_0\tau_c$ of 1.6 and 1.9 respectively ($\omega_0\tau_c$ of 1.12 leads to vanishment of nOe cross peaks). ROESY experiments which are more suitable for molecules of small size (MW $\leq$ 2000) were also performed but no additional information was obtained. As an alternative, the temperature dependence of ^1H and ^{31}P chemical shifts have been used to obtain qualitative information on the possible modes of stacking. The proton and phosphorus chemical shifts (data not shown) did not show any significant concentration dependence (< 0.02 ppm for ^1H and < 0.03 ppm for ^{31}P) indicating that no self-association occured at the concentrations used for the conformational study.

Table 3: ^1H- and ^{31}P-NMR chemical shifts (ppm, ^1H referenced to CH_3CN set at 2.00 ppm, ^{31}P referenced to cAMP set at 0.00 ppm) of **5** and **6** at 298 K in ^2H_2O.

		A^1	U^2	G^3	U^4	C^5	C^6	U^7
Self-cleaved hexamer **5**	H1'	6.11	5.70	5.84	5.81	5.86	5.76	
	H2'	5.23	4.15	5.15	4.34	4.20	4.35	
	H3'	4.90	4.50	4.96	4.55	4.26	4.43	
	H4'	4.49	4.16	4.25	4.39	4.26	4.20	
	H5'	4.20	4.00	3.92	4.25	4.19	3.87	
	H5"	4.02	3.95	3.92	4.13	4.07	3.76	
	H2	7.97	-	-	-	-	-	
	H8	8.21	-	7.71	-	-	-	
	H6	-	7.70	-	7.76	7.77	7.84	
	H5	-	5.75	-	5.79	5.85	5.99	
	2'P	0.29		21.4				
	3'P	0.75	0.75	21.4	0.90		0.75	
Self-cleaved heptamer **6**	H1'	6.25	5.82	5.99	5.96	6.02	6.01	5.92
	H2'	5.39	4.29	5.30	4.49	4.35	4.42	4.55
	H3'	5.06	4.62	5.11	4.70	4.42	4.67	4.64
	H4'	4.63	4.30	4.49	4.54	4.34	4.49	4.40
	H5'	4.35	4.12	4.09	4.49	4.23	4.42	4.03
	H5"	4.16	4.12	4.09	4.28	4.23	4.40	3.93
	H2	8.12	-	-	-	-	-	-
	H8	8.35	-	7.84	-	-	-	-
	H6	-	7.81	-	7.91	7.97	7.98	7.98
	H5	-	5.91	-	5.93	6.07	6.13	5.91
	2'P	0.26						
	3'P	0.67	0.84	21.4	0.89		0.74	0.67

(b) Conformation of the ribose:

In solution, the sugar ring exists in an equilibrium of two rapidly interconverting conformers denoted as C3'-*endo* (N) and C2'-*endo* (S). Two main approaches are available for the conformational analysis of the riboses. A detailed pseudorotational analysis in terms of phase angle of pseudorotation, puckering amplitude and population of S and N conformers requires the accurate determination of $J_{1'2'}$, $J_{2'3'}$ and $J_{3'4'}$ at several

Table 4: ^{1}H-^{1}H, ^{1}H-^{31}P and ^{13}C-^{31}P coupling constants (±0.25 Hz for J_{HH} and J_{HP} and ±0.5 Hz for J_{CP}) of **1** - **4** in $^{2}H_2O$. T = 298 K for **1**, **3** and **4** and T = 284 K for **2**.

		A[1]	U[2]	G[3]	U[4]	C[5]	C[6]	U[7]
Hexamer **1** A-form	$J_{1'2'}$	8.1	8.1	1.1	6.2	3.3	<2	
	$J_{2'3'}$	3.9	4.8	4.7	4.4	4.7	5.1	
	$J_{3'4'}$	2.3	2.2	7.3	3.8	a	7.9	
	$J_{4'5'}$	a	7.2b	3.6b	6.9b	2.3	a	
	$J_{4'5''}$	a				2.3	a	
	$J_{5'P5'}$	a	a	a	3.0	3.0	a	
	$J_{5''P5'}$	a	a	a	3.8	3.0	a	
	$J_{C1'P2'}$	2	-	-	-	-	-	
	$J_{C2'P3'}$		7.0	3	5.6	-	2	
	$J_{C3'P2'}$	6.9d	-	-	-	-	-	
	$J_{C4'P3'}$	9.9e	6.8e	11.9e	8.3e	-	a	
	$J_{C4'P5'}$					9.2		
Hexamer **1** B-form	$J_{1'2'}$	<2	7.5	7.0	3.6	3.0	6.6	
	$J_{2'3'}$	4.5	4.6	4.7	5.0	5.1	5.0	
	$J_{3'4'}$	8.1	2.0	1.8	a	a	2.0	
	$J_{4'5'}$	a	a	10.7b	a	a	6b	
	$J_{4'5''}$	a	a		a	a		
Heptamer **2**	$J_{1'2'}$	2.2	6.5	8.1	5.3	4.3	2.8	7.1
	$J_{2'3'}$	4.4	4.5	4.1	4.9	5.9	5.5	4.5
	$J_{3'4'}$	7.1	2.1	<1	5.1	5.6	7.4	2.8
	$J_{4'5'}$	2.0	6.2a	b	3.5	4.1	b	4.3a
	$J_{4'5''}$	4.2		b	3.0		b	
	$J_{5'P5'}$	3.0	3.1	b	3.0	3.0	6.0	b
	$J_{5''P5'}$	3.0	4.1	b	3.0	3.5	3.0	b
	$J_{2'P3'}$	-	1.1	2.2	-	-	-	-
cyclic A(2'→5')G tetramer **3**	$J_{1'2}$	4.8	7.4	1.5			1.1	
	$J_{2'3'}$	5.6	4.7	4.7			4.6	
	$J_{3'4'}$	4.2	1.7	7.6			8.9	
	$J_{4'5'}$	4.6	2.3	1.9			1.9	
	$J_{4'5''}$	4.1	a	1.3			1.3	
	$J_{2'P2'}$	8.1						
	$J_{3'P3'}$	8.0	7.8	9.8			6.7	
	$J_{5'P5'}$	6	7	4.5			3.3	
	$J_{5''P5'}$	3	3	2.2			2.7	
	$J_{C1'P2'}$	1.6						
	$J_{C2'P3'}$		6	<2			<2	
	$J_{C4'P3'}$ + $J_{C4'P5'}$	9.3	8.4	a			a	
cyclic A(3'→5')G tetramer **4**	$J_{1'2}$	7.1	6.9	3.8			2.7	
	$J_{2'3'}$	5.0	4.8	4.8			4.8	
	$J_{3'4'}$	1.5	2.4	5.9			6.6	
	$J_{4'5'}$	7.3	5.5	4.3			3.8	
	$J_{4'5''}$	2.9	2.2	4.1			2.9	
	$J_{2'P2'}$							
	$J_{3'P3'}$	8	8	8.4			7.8	
	$J_{5'P5'}$	3.8	6.3	4.7			4.5	
	$J_{5''P5'}$	3.0	2.0	3.1			4.0	
	$J_{C1'P2'}$							
	$J_{C2'P3'}$	3.6	4.3	5.4			<2	
	$J_{C4'P3'}$ + $J_{C4'P5'}$	2.5 (C4'-P3')	3.2 (C4'-P3')	5.7 (C4'-P3')			8.5 (C4'-P3')	

[a] Could not be measured due to spectral overlap, [b] $J_{4'5'} + J_{4'5''}$, [c] $J_{5'P} + J_{5''P}$, [d] $J_{C3'P2'} + J_{C3'P3'}$, [e] $J_{C4'P3'} + J_{C4'P5'}$

temperatures. In view of the fact that $J_{2'3'}$ and $J_{3'4'}$ are extracted from DQF-COSY and that the instability of **1** and **2** at high temperature (>25°C) prevented the measurement of the J-couplings, we have used the $J_{1'2'}$ coupling to calculate the population of N-type conformer according to the eqn. 1[26]:

$$\%N = 100 * (7.9 - J_{1'2'}) / 6.9 \quad .... \quad (1)$$

The results are summarized in Table 6 and show that **1-6** can be divided into two groups on the basis of the geometry of the ribose rings in the loop: (1) In the A-form of hexamer **1**, in **3** and **4**, the A^1 and U^2 residues are in the S-type conformation, while G^3 and C^6 are in the N-type conformation. (2) The second group consists of the B-form of hexamer **1** and heptamer **2**. In the B-form of **1**, A^1 adopts the N-type conformation, while U^2 and G^3 have a South geometry. In **2**, A^1 is also in the N-type conformation whereas U^2 and G^3 are in the South conformation. In the B-form of **1**, the C^6 residue which is linked through its 5'-phosphate to the 3'-hydroxyl of G^3 is in the S-type conformation. In the heptamer, the U^7 residue which is linked through its 5'-phosphate to the 3'-hydroxyl of G^3 also adopts the S conformation. The N⇄S equilibrium in lariat RNAs **1-2** was found to be insensitive to changes in temperature. On the other hand, in the cyclic tetramers **3** and **4**, an increase of temperature strongly affects the sugar ring population of G^3 and C^6. Thus at 5°C, G^3 and C^6 in **3** show a strong preference for the N-type conformation (*ca.* 100% N), but at 70°C, they show around 55 % of N conformers. A^1 and U^2 are much less affected by an increase of temperature and their population change from 67% S for A^1 and 97% S for U^2 at 5°C to 46% S and 89% S respectively at 70°C. In **4**, G^3 and C^6 are in a pure N-type conformation, while at 70°C, they show 43% and 29% of North conformers. The sugar rings of A^1 and U^2 are, as in **3**, less sensitive to an increase of temperature.

Table 5: ^1H-^1H and ^1H-^{31}P coupling constants (±0.25 Hz) for the self-cleaved hexamer **5** and heptamer **6** at 298K in ^2H_2O.

		A^1	U^2	G^3	U^4	C^5	C^6	
Self-cleaved Hexamer **5**	$J_{1'2'}$	4.6	5.8	4.1	5.6	3.6	3.0	
	$J_{2'3'}$	4.9	5.4	7.1	4.6	5.5	5.1	
	$J_{3'4'}$	5.3	3.7	4.1	4.5	a	7.1	
	$J_{4'5'}$	5.9	3.0	7.1	3.0	a	3.0	
	$J_{4'5''}$		3.1		4.1	a	4.1	
	$J_{3'P3'}$	8.2	7.2	8.1	8.2	a	8.1	
	$J_{5'P5'}$	a	4.1	a	4.1	a	a	
	$J_{5''P5'}$	a	3.1	a	4.0	a	a	
Self-cleaved Heptamer **6**	$J_{1'2'}$	4.2	6.0	3.9	5.1	4.1	4.4	4.9
	$J_{2'3'}$	4.9	5.2	7.1	5.1	5.0	4.7	5.1
	$J_{3'4'}$	5.3	3.5	4.5	4.0	4.0	a	6.1
	$J_{4'5'}$	3.9	a	4.1	4.1	3.0	a	2.9
	$J_{4'5''}$		a		4.1	4.1	a	4.1
	$J_{3'P3'}$	a	8.1	a	a	a	a	8.1
	$J_{5'P5'}$	a	a	7.0	a	3	a	a
	$J_{5''P5'}$	a	a		a	3.5	a	a

[a] could not be measured because of spectral overlap

(c) Glycosidic bond conformation:

A nucleotide with a N-type sugar has an *anti* conformation when a strong nOe between the H8/H6 and H3' together with a weak or a complete absence of nOe between the H8/H6 and H1' is observed. For a S-type sugar, the *anti* conformation is preferred if a strong nOe between H8/H6 and H2' is observed. If these intensities are reversed, the *syn* conformation is favoured. The data for **1-6** are summarised in Table 6. *Hexamer A-form*: The H8 of A^1 had a strong nOe with its H2' and a weak nOe with its H1' indicating an *anti*

conformation. The H8 of G^3 showed a weak nOe cross peak with its H2'. No nOe between H8 and H3' was observed despite the N conformation of the ribose. This is due to the fact that the H3' of G^3 has the same chemical shift that the residual HOD peak (4.7 ppm), which is preirradiated during the mixing time. However, because of the absence of H8-H1' cross peak, one can conclude that G^3 is probably in the *anti* conformation. *Hexamer B-form*: The H8 of A^1 showed an nOe cross peak only with its H1' indicating a *syn* conformation. A qualitative inspection of the NOESY spectrum did not show any cross peak for the G^3 residue. It should be noted that at 25° C, the B form accounts for only 25% of the conformer population which means that the nOe cross peaks are expected to be very weak. By taking a 1D projection along the H8 of G^3, one could however observe nOe between H8-H2' and H8-H1'. The integration of these nOe cross peaks suggests that the G^3 is in the *syn* conformation. *Heptamer*: The H8 of A^1 had a strong nOe with its H1' implying a *syn* conformation. G^3 also showed a strong nOe between H8 and H1' indicating a *syn* orientation of the base. The pyrimidine nucleotides were found to adopt the *anti* conformation in all compounds.

Table 6: Conformational properties (% North, γ^+ and β^t rotamers, orientation of the glycosidic bond χ and preferred conformation around the C3'-O3' bond ε; error ± 10%) in **1** - **6**.(T = 298 K in **1**, **5** and **6**. T = 284 K in **2** and T = 278 K in **3** and **4**).

		A^1	U^2	G^3	U^4	C^5	C^6	U^7
Hexamer **1** A-form	%N	0	0	100	25	67	100	
	χ	*anti*	*anti*	*anti*	*anti*	*anti*	*anti*	
	$\%\gamma^+$	d	63	100	66	90	d	
	$\%\beta^t$	d	d	β^t	91	95	d	
	ε	ε^-	ε^-	ε^t	$\varepsilon^-, \varepsilon^t$		ε^t	
Hexamer **1** B-form	%N	100	7	13	62	71	19	
	χ	*syn*	*anti*	*syn*	*anti*	*anti*	*anti*	
	$\%\gamma^+$	d	d	27	d	d	75	
	$\%\beta^t$	d	d	d	d	d	d	
	ε	d	d	d	d	d	d	
Heptamer **2**	%N	83	20	0	38	52	71	12
	χ	*syn*	*anti*	*syn*	*anti*	*anti*	*anti*	*anti*
	$\%\gamma^+$	73	73	d	70	75	d	93
	$\%\beta^t$	95	88	d	95	80	93	d
	ε		ε^-	ε^-	d	d	d	d
A(2'→5')G linked Tetramer **3**	%N	33	3	100			100	
	χ	*anti*	*anti*	*syn*			*anti*	
	$\%\gamma^+$	47	d	100			100	
	$\%\beta^t$	80	76	92			95	
	ε	ε^t	ε^-	ε^t			ε^t	
A(3'→5')G linked Tetramer **4**	%N	0	0	100			100	
	χ	*anti*	*anti*	*syn*			*anti*	
	$\%\gamma^+$	32	58	50			68	
	$\%\beta^t$	91	84	86			83	
	ε	ε^t	$\varepsilon^-, \varepsilon^t$	$\varepsilon^-, \varepsilon^t$			ε^t	
Self-cleaved Hexamer **5**	%N	48	30	51	33	62	71	
	χ	*anti*	*anti*	a	*anti*	*anti*	*anti*	
	$\%\gamma^+$	76	74	65	65	d	64	
	$\%\beta^t$	d	89	d	85	d	d	
	ε	d	d	d	d	d	d	
Self-cleaved Heptamer **6**	%N	54	27	58	40	55	51	43
	χ	*anti*	*anti*	a	*anti*	*anti*	*anti*	*anti*
	$\%\gamma^+$	96	d	95	52	64	d	65
	$\%\beta^t$	d	d	90	d	90	d	d
	ε	d	d	d	d	d	d	d

[a] Calculated using equation (1), [b] calculated using equation (2), [c] calculated using equation (3), [d] could not be determined.

(d) Backbone conformation:

The coupling constants necessary to define the conformation of the phosphate backbone have been measured from 2D DQF-COSY ($^3J_{HH}$, $^3J_{HP}$), from 1D $^{13}C\{^1H\}$ spectra ($^3J_{CP}$), and from 2D heteronuclear proton-carbon correlation experiment HSQC[27] ($^3J_{HP}$, $^3J_{CP}$). Since in most cases only the sum $J_{4'5'} + J_{4'5''}$ was available, the population of *gauche*$^+$ conformer (Table 6) around the C4'-C5' bond (γ) was calculated using eqn. 2[28]:

$$\%\gamma^+ = 100 * (13.3 - J_{4'5'} - J_{4'5''}) / 9.7 \quad .... \quad (2)$$

The amount of *trans* conformer (Table 6) around the C5'-O5' bond (β) was estimated from the values of the $J_{5'P}$ and $J_{5''P}$ using the eqn. 3[29]:

$$\%\beta^t = 100 * (25.5 - J_{5'P} - J_{5''P}) / 20.5 \quad .... \quad (3)$$

Because of the crowding of the H3'/4'/5'/5" region, all the $J_{4'5'}$, $J_{4'5''}$, $J_{5'P}$ and $J_{5''P}$ could not be measured from the DQF-COSY. The problem was particularly crucial for the B-form of **1**, since it accounts for only 25% of the hexamer at 25°C. *Hexamer, A-form*: The U^2, G^3, U^4 and C^5 residues are in the γ^+ conformation. No information could be obtained for A^1 and C^6. The amount of β^t conformer could be calculated only for the U^4 and C^5 residues. These two nucleotides show a strong preference for the β^t population (> 90%). A $^4J_{H4'P}$ of 2.3 Hz was measured from the H4'-H3' DQF-COSY cross peak of G^3. This long range coupling is possible only for a W-path *i.e.* for a planar H4'-C4'-C5'-O5'-P geometry, which occurs with the β^t conformation. *Hexamer B form*: The γ^+ population was determined only for G^3 and C^6 residues. The C^6 residue adopt the γ^+ conformation (75%), but the G^3 residue shows only 27% of γ^+ rotamer. We could not discriminate between γ^- and γ^t conformation since only the sum $J_{4'5'} + J_{4'5''}$ was available. None of the $J_{5'P}$ and $J_{5''P}$ coupling constants could be measured. *Heptamer*: The population of γ^+ and β^t conformers could be estimated for A^1, U^2, U^4 and C^6. All nucleotides preferred the γ^+ and β^t conformation ($\gamma^+ > 70\%$ and $\beta^t > 80\%$). *A(2'→5')G and A(3'→5')G linked tetramers 3 and 4*: Table 5 shows that it is only C^6 residue in **3** and **4** which adopts γ^+ orientation around the C4'-C5' bond while all residues in these RNAs adopt β^t conformation around the C5'-O5' bond.

The conformation about the C3'-O3' bond (ε) is monitored by the $J_{H3'P3'}$, $J_{C2'P3'}$ and $J_{C4'P3'}$[29,30] Since $J_{H3'P3'}$ is nearly identical for the two rotamers ε^t and ε^-, it cannot be used alone to distinguish between the two conformations. In 3'→5' oligonucleotides, the expected magnitude of $J_{C4'P3'}$ and $J_{C2'P3'}$ for a pure ε^- conformation is 0.5 Hz and 9.4 Hz ($\varepsilon = 275°$). For a pure ε^t conformation, they are 7.4 and 1.4 Hz respectively ($\varepsilon = 219°$). *Hexamer 1 A-form*: Table 3 shows that the U^2 residue has a large $J_{C2'P3'}$ coupling of 7 Hz which indicates a preference for the ε^- conformation. The G^3 and C^6 residues have small $J_{C2'P3'}$ couplings (3 and 2 Hz respectively), suggesting that they may prefer the ε^t conformation. However, since the $J_{C4'P3'}$ could not be determined unambiguously, the conformational assignment is not certain. For the U^4 residue, the value of 5.6 Hz for the $J_{C2'P3'}$ indicates that the C3'-O3' bond is in an equilibrium between ε^- and ε^t conformation. The adenosine branch-point A^1 shows a large sum $J_{C2'P3'} + J_{C2'P2'}$ and a smaller sum $J_{C4'P3'} + J_{C4'P5'}$ suggesting a preference for the ε^-conformation. The ε^- conformation of A^1 was confirmed by the detection of a long range $^4J_{H2'P3'}$ coupling. This long range coupling is only possible along a planar W-path created when the sugar ring adopts an S-type conformation and the C3'-O3' bond an ε^- conformation[30]. *Heptamer 2*: The sample concentration was too low to allow the measurement of ^{13}C-^{31}P coupling constants from ^1H-^{13}C correlation experiment. In the DQF-COSY, the detection of a long range $^4J_{H2'P3'}$ for the U^2 and G^3 residues indicates a ε^- conformation about the C3'-O3' bond. As $J_{C4'P3'}$ and $J_{C2'P3'}$ provide information on the C3'-O3' conformation, the $J_{C1'P2'}$ and $J_{C3'P2'}$ can give information on the conformational preference around C2'-O2'. A large $J_{C1'P2'}$

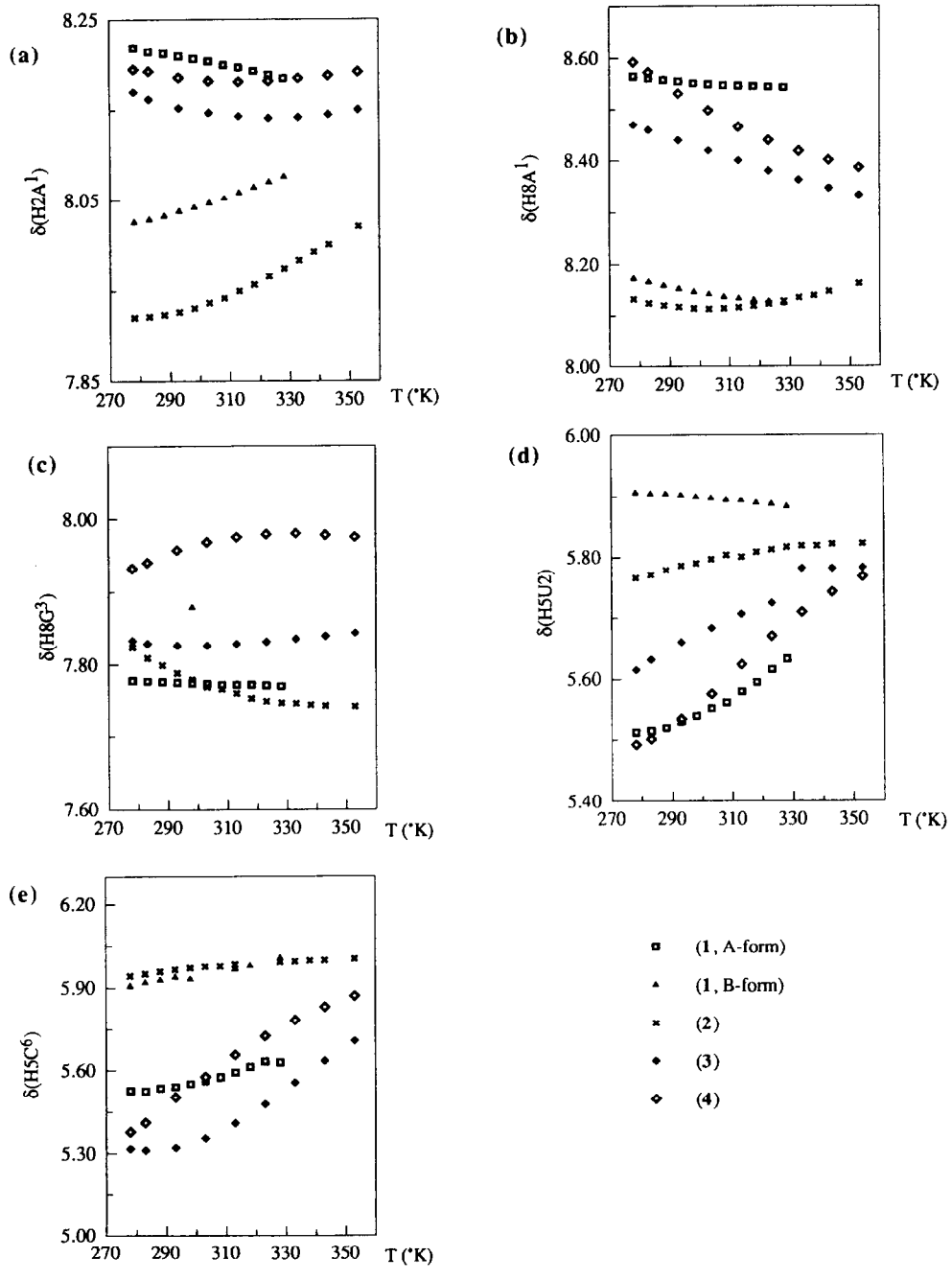

Figure 5: ^{1}H-NMR chemical shifts (δ, ppm) *vs.* temperature (K) for: (a) H2A^{1}, (b) H8A^{1}, (c) H8G^{3}, (d) H5U^{2} and (e) H5C^{6}.

and small $J_{C3'P2'}$ indicates a high population of ε^- conformer. Thus, in **1**, the A^1 residue adopts preferentially the ε^- conformation about the C2'-O2' bond. *A(2'→5')G and A(3'→5')G linked tetramers 3 and 4*: In **3** the U^2 residue has a large $^3J_{C2'P3'}$ coupling (6 Hz) which indicates that the C3'-O3' is mainly in the ε^- conformation. G^3 and C^6 on the other hand have a small $^3J_{C2'P3'}$ (<2 Hz) suggesting a preference for the ε^t conformation. The A^1 residue has a small $^3J_{C1'P2'}$ (1.6 Hz) and adopts mainly the ε^t conformation around the C2'-O2' bond. In **4**, the small $^3J_{C2'P3'}$ (< 2 Hz) for A^1 suggest a preference for the ε^t geometry. The C^6 residue has a large $^3J_{C4'P3'}$ and small $^3J_{C2'P3'}$ indicating a high population of ε^t conformer. For the U^2 and G^3 residues, the intermediate $^3J_{C4'P3'}$ and $^3J_{C2'P3'}$ suggest that the C3'-O3' bond is equally populated with ε^- and ε^t rotamers.

(e) ^{1}H-NMR chemical shift to assess the intramolecular base-base stacking.:

Inspection of Table 2 and Figure 5 shows that RNAs **1-4** can be divided into two groups based on their relative chemical shifts and the temperature dependency of chemical shifts: (I) hexamer **1** B-form and heptamer **2**, and (II) hexamer **1** A-form, **3** and **4**. At 278K, the H8 and $H2A^1$ in **1** B-form and **2** are more shielded than those in the A-form of hexamer **1**, **3** and **4**. This difference in chemical shifts for A^1 can be partially due to change in the ribose and glycosidic bond conformation, but may also reflect a different influence of the neighbouring nucleotides. The $H5C^6$ and $H5U^2$ are more deshielded in the B-form of hexamer **1** and heptamer **2** than in the A-form of hexamer **1**, **3** and **4**. The $H5U^4$ is also more deshielded in the A-form than in the B-form of hexamer **1**. The dissimilar behaviour of the $H6U^2$ and $H6C^6$ residues in the loop and $H6U^4$ in the tail in A- and B-form of hexamer **1** also reflect a different influence of the stereochemical environment. Upon an increase of temperature from 278 K to 353 K, the $H8A^1$ in the A-form of **1**, **3** and **4** are found to be shielded whereas the $H5U^2$ and $H6C^6$ are deshielded. The conformation of **3** and **4** are particularly sensitive to temperature changes. The deshielding of $H6U^2$ can be attributed either to the influence of the A^1 or C^6 residues. Since a uridine base has only a small ring current effect, the deshielding of $H6C^6$ might be due to the ring current effect of G^3. In the heptamer **2** and the B-form of hexamer **1**, it is the $H2A^1$ and $H8G^3$ which experience a downfield and upfield shifts, respectively, upon an increase of temperature. These data suggest that several weakly stacked and unstacked conformations in equilibrium may exist in solution in **1-6**. In the A-form of hexamer **1** as well as in **3** and **4**, the loop nucleotides A^1, U^2, G^3 and C^6 are probably involved in some stacking interactions, while the 3'-tail nucleotides are apart. These data also suggest that A^1, G^3 and U^4 nucleobases in the B-form of hexamer **1** and heptamer **2** could be also weakly interacting.

Thermodynamics and kinetics of the two exchanging "A" ⇄ "B" forms of lariat hexamer 1.

To the best of our knowledge, this is the first report of a single stranded circular RNA which has been found to have two slowly exchanging conformations on the NMR time scale. Transition between double-stranded A-RNA and Z-RNA[31] and between double-stranded B-DNA and Z-DNA[32,33] have been however observed by NMR. It has also been shown that RNA pseudoknot and hairpin structure are in slow equilibrium on the NMR time scale, the position of the equilibrium however depends on the ionic strength, temperature, sequence and size of the loop[34]. The transition between right-handed and left-handed helix requires considerable changes in the backbone conformation and particularly, in the phosphodiester torsional angles. In addition, the sugar puckering and the orientation of the base relative to the sugar are different. In B-DNA, the guanosine and cytidine residues have C2'-*endo*, *anti* conformation. In Z-DNA, guanosine is in the

C3'-*endo*, *syn* conformation. The phosphodiesters torsion α and ξ move from g^-, g^- conformation to g^+, g^+ conformation for the pyrimidine-purine step and g^-, g^t conformation for the purine-pyrimidine step. In A-RNA, the guanosine and cytidine residues have a C3'-*endo* conformation and an *anti* orientation of the base about the glycosidic bond. In Z-RNA, the G residues are in the C3'-*endo*, *syn* conformation while the C residues are in the C2'-*endo*, *anti* conformation.

(a) Thermodynamics:

The relative intensities of the aromatic H2 and anomeric H1' resonances of adenosine A^1 in **1** were used to calculate the equilibrium constant for the transition between the two slowly exchanging forms. The other aromatic and anomeric resonances could not be used due to the crowding of the spectra. The intensity of a resonance is proportional to the population of the particular conformer at a certain temperature. The ratio of the intensities H2A^1(B-form)/H2A^1(A-form) at eight temperatures between 5°C and 45°C were used to calculate the equilibrium constants K ($K = x_B/x_A$ where x_B/x_A is the fraction of B-conformer versus A-conformer). At 5°C, the equilibrium constant for the formation of the B-form from the A-form is 0.1 and at 45°C, it is 0.75. From the plot of $\ln(x_B/x_A)$ versus 1/T, an enthalpy of transition ΔH of 7.1 ± 0.6 kcal.mol^{-1} and an entropy of transition ΔS of 21 ± 1.1 cal.mol^{-1}.K^{-1} were calculated. Despite the error in the calculation, due to difficulties in obtaining accurate integration of resonances, these data indicate that the enthalpy term favors the A-form, while the entropy term favors the B-form conformation. This is consistent with the NMR observation that the A-form is predominant at low temperature and it has probably a more rigid conformation than the B-form which is perhaps more flexible.

(b) Kinetics:

The rate of exchange between the two slowly exchanging systems A and B was determined by cross saturation experiments[35-37] in which one of a pair of exchanging resonances is selectively saturated and the effect on the other resonances is monitored: We chose to irradiate the H2 resonance of adenosine A^1 in the saturation transfer experiment. The H2 resonances are singlets, they are in a relatively uncrowded region of the spectrum, and they are well enough separated from each other so that selective irradiation can be achieved without disturbing the neighbouring resonances. Also, the relaxation time T_1 of H2(A^1) is found to be sufficiently long [T_1 of H2(A^1) in A form = 1.9s and T_1 of H2(A^1) in B form = 1.5s] to allow a longer linear build up of transferred magnetization to occur before the longitudinal relaxation. The H2 of A^1 in the B-form was irradiated, and the exchange transfer to H2 of A^1 in the A-form was observed. The ratio of the intensity of the H2(A^1) of the A-form in the difference spectrum to the intensity of the H2(A^1) of the A-form in the control spectrum gave the amount of transfer of magnetization. The magnitude of exchange transfer as a function of irradiation time was used to calculate the rate of exchange at different temperatures[38]. The energy of activation, E_a, was then determined from the temperature dependence of the rate constants. The Arrhenius plot $\ln(k_a/(k_a+\rho)) = f(1/T)$ gave an activation energy of 23.8 ± 1.8 kcal.mol^{-1}. The activation parameters for the A-form to B-form transition are $\Delta H^{\#}$ = 23 kcal.mol^{-1} and $\Delta S^{\#}$ = 15.6 cal.mol^{-1}.K^{-1}. The free energy of activation is 18 kcal.mol^{-1} at 25°C. The same experiment was performed with the triethylammonium salt of the hexamer, and an activation energy E_a of 21.8 ± 2.2 kcal. mol^{-1} was determined. Since the cyclic A(2→5')G tetramer **3** exhibits only one average conformation on the NMR time scale, the barrier to interconversion between the A- and B-form in hexamer **1** must be due to the 3'-tail nucleotides attached to the adenosine branch-point A^1.

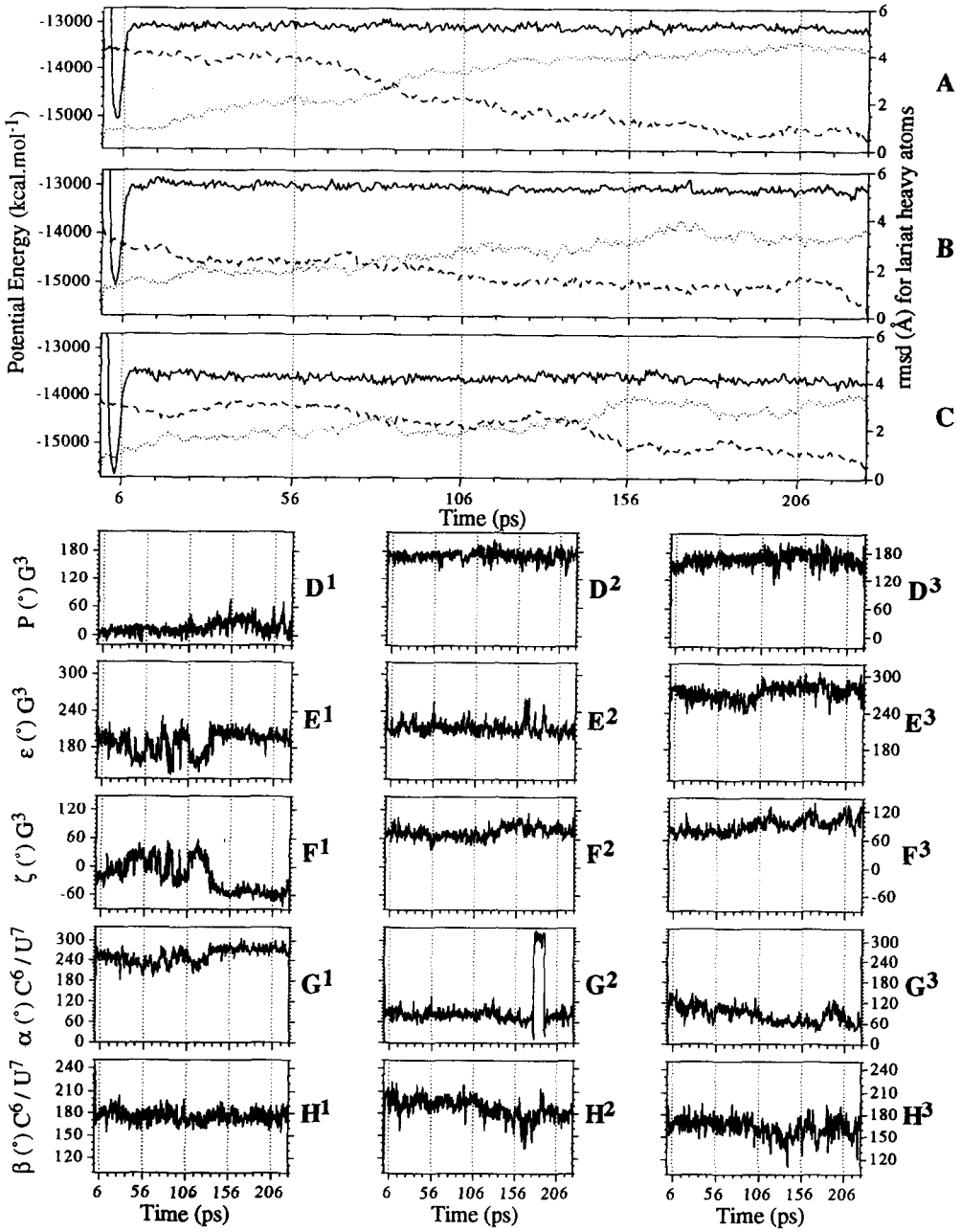

Figure 6: Panels (A)-(C) show the evolution of potential energies over the 226 ps MD simulations in water (left scale, solid lines) for A-form of hexamer 1 (panel A), B-form of hexamer 1 (panel B) and heptamer 2 (panel C), they also show the rmsd in Å (right scale, non-solid lines) for the heavy atoms (water-oxygens and sodium ions were not included in rmsd calculations). The dotted lines correspond to the rmsd relative to the initial structure obtained from the *in vacuo* conformational search procedure[39], the broken lines correspond to the rmsd relative to the structures obtained at 226 ps. Panels (D)-(H) show the variation of the phase angle (P), ε, ζ, α, and β torsions of the G^3 and C^6/U^7 residues at the self-cleavage site during the total MD simulations in water. The left column corresponds to the A-form of hexamer 1, the middle column to the B-form of hexamer 1, and the right column to the heptamer 2.

Molecular dynamics simulation of lariat-RNAs in water for 226 ps at 284K

The low energy conformers obtained from a conformational search procedure in vacuum[39] were found to be stabilized by various intramolecular hydrogen bonds, particularly to the phosphate oxygens, and a few stacking interactions (G^3-C^6 in hexamer **1** A-form, A^1-G^3-C^5 in hexamer **1** B-form, and in heptamer **2**). The lowest energy lariat-RNA structures from the conformational search procedure[39] in vacuum were immersed in a periodic box of water[40] and the three solvated systems were subjected to 226 ps of MD simulation. The MD simulations were first carried out with harmonic constraints which were derived from the NMR-data (0-96 ps) and then completely without constraints (106-226 ps). Torsional constraints were only imposed on torsions where NMR-data showed that the preference for one rotamer exceeded ~70 %. Additionally, the constraining harmonic potential wells have a flat bottom (see Table 7) and the width of the flat bottom would for most torsions allow large torsional movements within the NMR-obeyed torsional space.

Table 7: The constrained torsions with the target dihedral angle and the allowed variation in degrees, and the force constant in kcal.rad^{-2}. The harmonic potential for the constraints have a flat bottom, its width given by the allowed variation, and the force constants for the regions outside the allowed variation is the same for both lower side and higher side.

Hexamer 1. A-form	G^3	C^6	U^2	A^1	U^4	C^5		Force constant
ν_0	9.6 ±8	9.6 ±8	-22.8 ±8	-22.8 ±8	-22.8 ±8	-		150
ν_2	37.0 ±8	37.0 ±8	-34.8 ±8	-34.8 ±8	-34.8 ±8	-		150
β	180.0 ±60	180.0 ±60	-	180.0 ±60	180.0 ±60	180.0 ±60		150
γ	60.0 ±40	-	-	-	-	60.0 ±40		150
ε	240.0 ±120	-	300.0 ±60	300.0 ±60	240.0 ±120	-		150
χ	180.0 ±90	180.0 ±90	180.0 ±90	180.0 ±90	180.0 ±90	180.0 ±90		50
Hexamer 1. B-form	G^3	C^6	U^2	A^1	U^4	C^5		Force constant
ν_0	-22.8 ±8	-22.8 ±8	-22.8 ±8	9.6 ±8	-	-		150
ν_2	-34.8 ±8	-34.8 ±8	-34.8 ±8	37.0 ±8	-	-		150
γ	-	60.0 ±40	-	-	-	-		150
ε	-	300.0 ±60	-	-	-	-		150
χ	0.0 ±90	180.0 ±90	180.0 ±90	0.0 ±90	180.0 ±90	180.0 ±90		50
Heptamer 2.	G^3	U^7	C^6	U^2	A^1	U^4	C^5	Force constant
ν_0	-22.8 ±8	-22.8 ±8	-	-22.8 ±8	9.6 ±8	-	9.6 ±8	150
ν_2	-34.8 ±8	-34.8 ±8	-	-34.8 ±8	37.0 ±8	-	37.0 ±8	150
β	-	-	180.0 ±60	180.0 ±60	180.0 ±60	180.0 ±60	180.0 ±60	150
γ	-	60.0 ±40	60.0 ±40	60.0 ±40	60.0 ±40	60.0 ±40	-	150
ε	300.0 ±60	-	-	300.0 ±60	-	-	-	150
χ	0.0 ±90	180.0 ±90	180.0 ±90	180.0 ±90	0.0 ±90	180.0 ±90	180.0 ±90	50

For all three RNA structures noticeable changes in conformation occurred already after 10-30 picoseconds of MD simulation in water (panels A-C in Fig. 6 for rmsd and potential energy of structures along the 226 ps MD trajectory). The conformations of the three structures did not, however, change dramatically when the torsional constraints were released (panels A-C in Fig. 6). The sugar conformation of C^6 in B-form

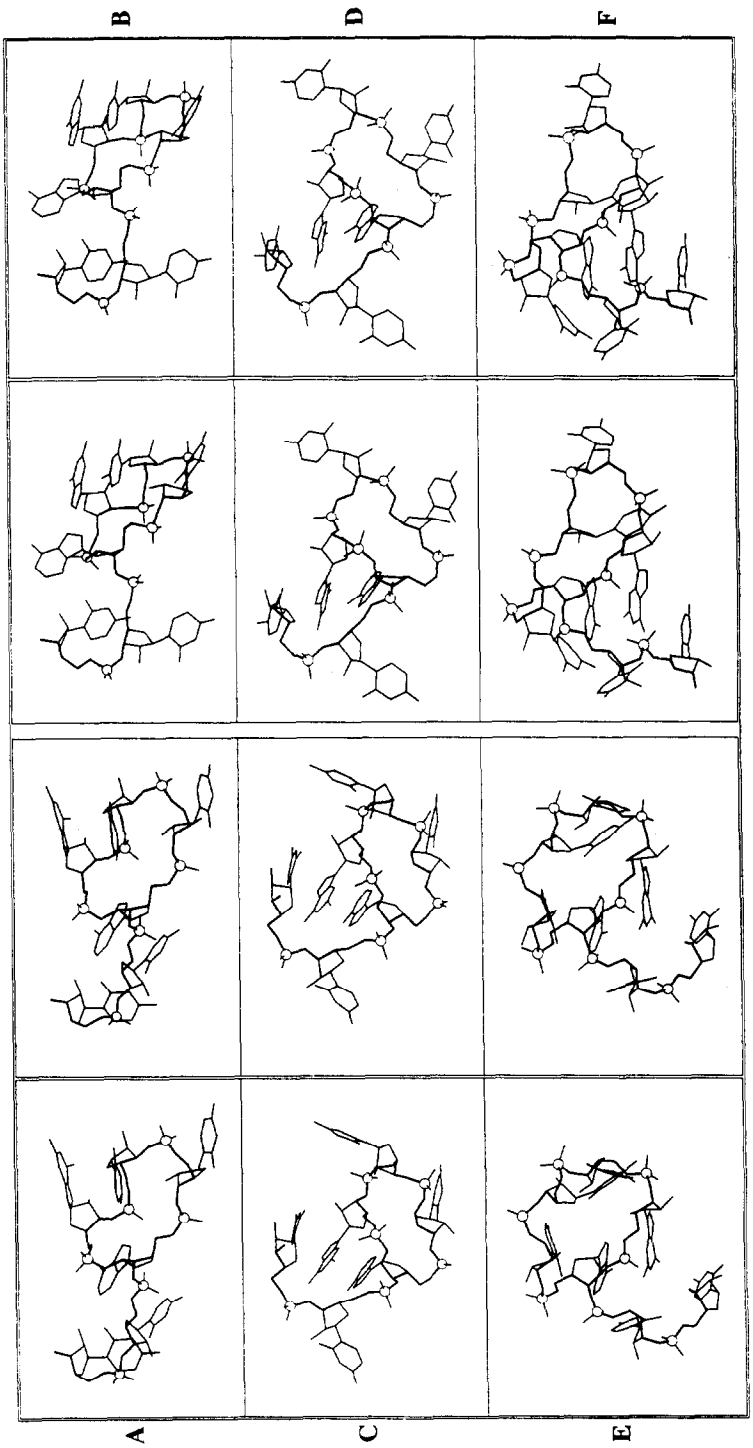

Figure 7: The stereoviews of the cyclic branched RNAs from the snapshots at 96 ps (the last fully NMR constrained structure) and at 226 ps (the last unconstrained structure) from the MD simulation in water at 284K (see ref. 40). All water molecules, sodium ions, and hydrogen atoms have been omitted for clarity. All phosphorus atoms are shown as open circles and the phosphate backbone is shown with thick lines. Panel (A): Hexamer 1 A-form at 96 ps . Panel (B): Hexamer 1 A-form at 226 ps. Panel (C): Hexamer 1 B-form at 96 ps. Panel (D): Hexamer 1 B-form at 226 ps. Panel (E): Heptamer 2 at 96 ps. Panel (F): Heptamer 2 at 226 ps. See Figs. 6 and 8 for variation of sugar-phosphate backbone for structures for the entire trajectory.

of hexamer **1** switched from South to North but the global conformation remained essentially the same (panel B for rmsd in Fig. 6) despite this change in sugar conformation at ~100 picoseconds. A similar conclusion can also be reached from a comparison of NMR-constrained (Table 7) and unconstrained conformers in panels C and D in Fig. 7. The lack of any major changes in the conformation of the three lariat-RNA structures indicate that the conformers generated in the MD simulation in water agree well with the NMR-derived structural features (Tables 6 and 7). The ensemble of conformers generated during the MD trajectory of 226 picoseconds are not artificially held in these conformations due to the NMR constraints, and they may (Fig. 7 for stereoviews at 96 and 226 picoseconds) be considered as good representatives of the actual NMR observed solution structures. The low number of constraints due to the limited number of experimental observables do not allow a more precise structure determination and other low energy structures may also be in agreement with the present NMR data. Fig. 8 shows the scatter plots depicting the variation of different sugar-phosphate backbone torsions for structures snapshot at every 0.5 ps from the entire 226 ps in water in both NMR constrained and unconstrained modes.

The conformation of the sugar-phosphate backbone of the three lariat-RNA structures at the site of self-cleavage between G^3 and C^6/U^7 residues is of particular interest since it is the 3'-phosphate of G^3 that undergoes a transesterification reaction by the vicinal 2'-OH to give a trigonal bipyramidal phosphate as a transition state/intermediate which upon displacement of the 5'-oxygen gives a 2',3'-cyclic phosphate (G^3) and a 5'-hydroxy terminus (C^6/U^7). Several similarities can be seen among the torsions of the B-form of hexamer **1** and the heptamer **2** (Figs. 6-9). The A-form of the hexamer **1** is on the other hand quite different partly due to the fact that the sugar conformation of the G^3 residue is North while it is South in the other two structures. The average distances between the O2' of the G^3 residue and the phosphorus atom of the vicinal 3'-phosphate is 3.5, 3.3, and 4.0 Å for hexamer A-, and B-forms, and heptamer respectively (Fig. 9 for the stereoviews of the cleavage-site). Model building studies suggest that the ε-torsion of the G^3 residue should be close to 120° for the O2'-P bond to form in the transesterification step and the ζ-torsion should be close to 180° to position the O5' of the C^6/U^7 residue for its in-line displacement by the incoming O2' nucleophile. The torsions in our three lariat-RNA structures would need to change from $\varepsilon^{t/-}$ to $\varepsilon \approx 120°$ and from $\zeta^{-/+}$ to $\zeta \approx 180°$, which would result in a distance $d_{O2'\text{-}3'P}$ of ~2.8 Å. The α torsion in the B-form of hexamer and heptamer are found to be α^+ whereas for the A-form of hexamer it is α^-. Such a structure might serve as a precursor for the in-line attack by the 2'-OH group for the formation of the trigonal bipyramidal phosphorane geometry. This is consistent with studies made by us[9] and others[41] on the *ab initio* optimized geometries of cyclic oxyphosphoranes as models of the intermediate in splicing and cleavage of RNA (Gaussian 92 HF/3-21G basis set) which show the following geometry for the trigonal bipyramidal intermediate or the transition state: $\varepsilon = +110°$, $\zeta = -178°$, $\alpha = 66°$, $d_{O2'\text{-}3'P} = 1.8$ Å.

Conclusion

The uncatalyzed rate of cleavage of a RNA phosphodiester bond by a weak nucleophile such as 2'-OH or H_2O has been estimated to be less than 10^{-7} min^{-1}. The rates observed for our systems ($k = 0.25\ 10^{-4}$ min^{-1} for **1**, $k = 0.16\ 10^{-3}$ min^{-1} for **2**) must then be due to intrinsic molecular features. Even if none of the nucleotides normally have pKas in the neutral pH range in which the rate of cleavage is the highest, an acid and base function could be provided by the functional group of a nucleotide for which the pK_a has shifted due

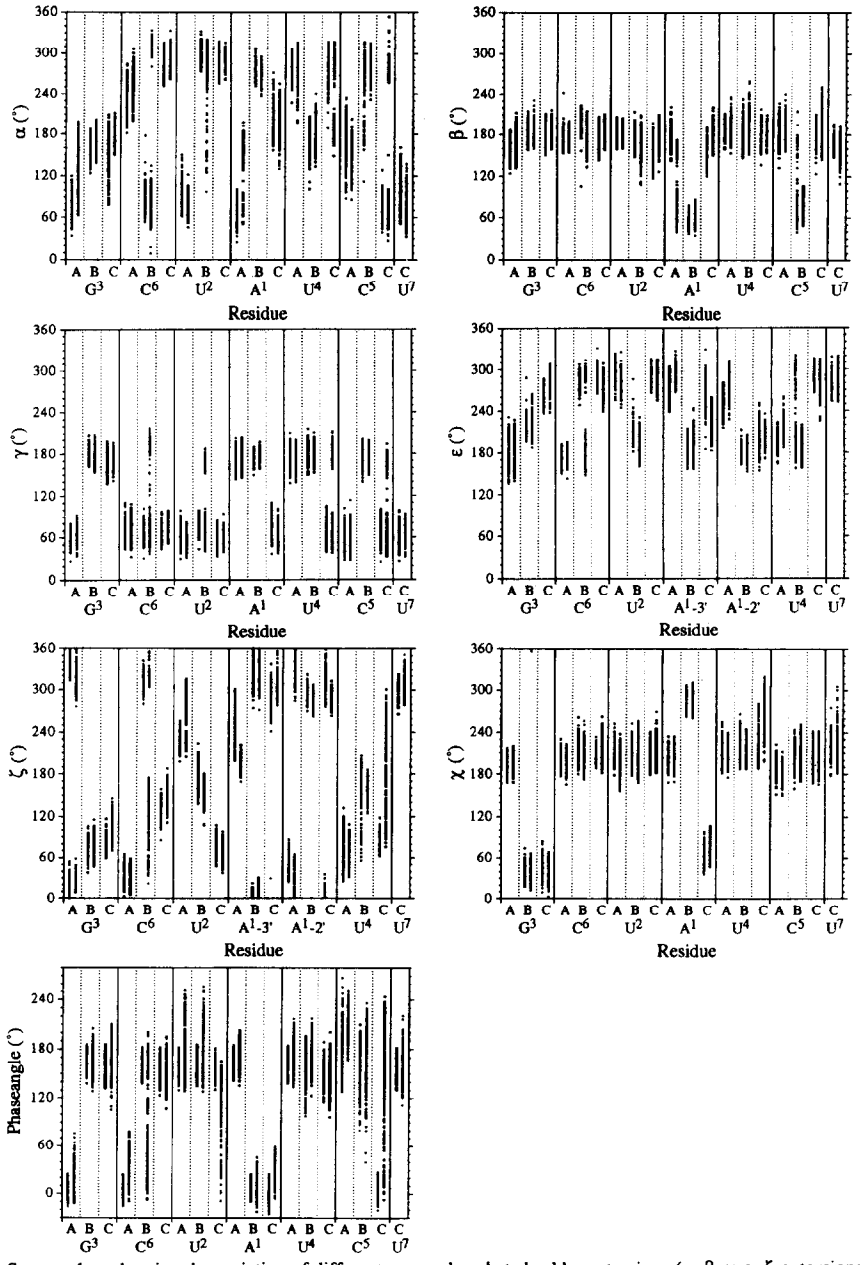

Figure 8: Scatter plots showing the variation of different sugar-phosphate backbone torsions (α, β, γ, ε, ζ, χ torsions and phase angles (P)) for structures sampled every 0.5 ps from the entire 226 ps MD simulations in water in both NMR constrained and unconstrained modes. The rectangular boxes subtitled (A) represent variations of torsions for the A-form of hexamer 1: left lane in (A) represents NMR constrained part (0-96 ps) of the MD and the right lane in (A) represents the unconstrained part (96-226 ps) of the MD. The rectangular boxes subtitled (B) represent variations of torsions for the B-form of hexamer 1: left lane in (B) represents NMR constrained part (0-96 ps) of the MD and the right lane in (B) represents the unconstrained part (96-226 ps) of the MD. The rectangular boxes subtitled (C) represent variations of torsions for the heptamer 2: left lane in (C) represents NMR constrained part (0-96 ps) of the MD and the right lane in (C) represents the unconstrained part (96-226 ps) of the MD.

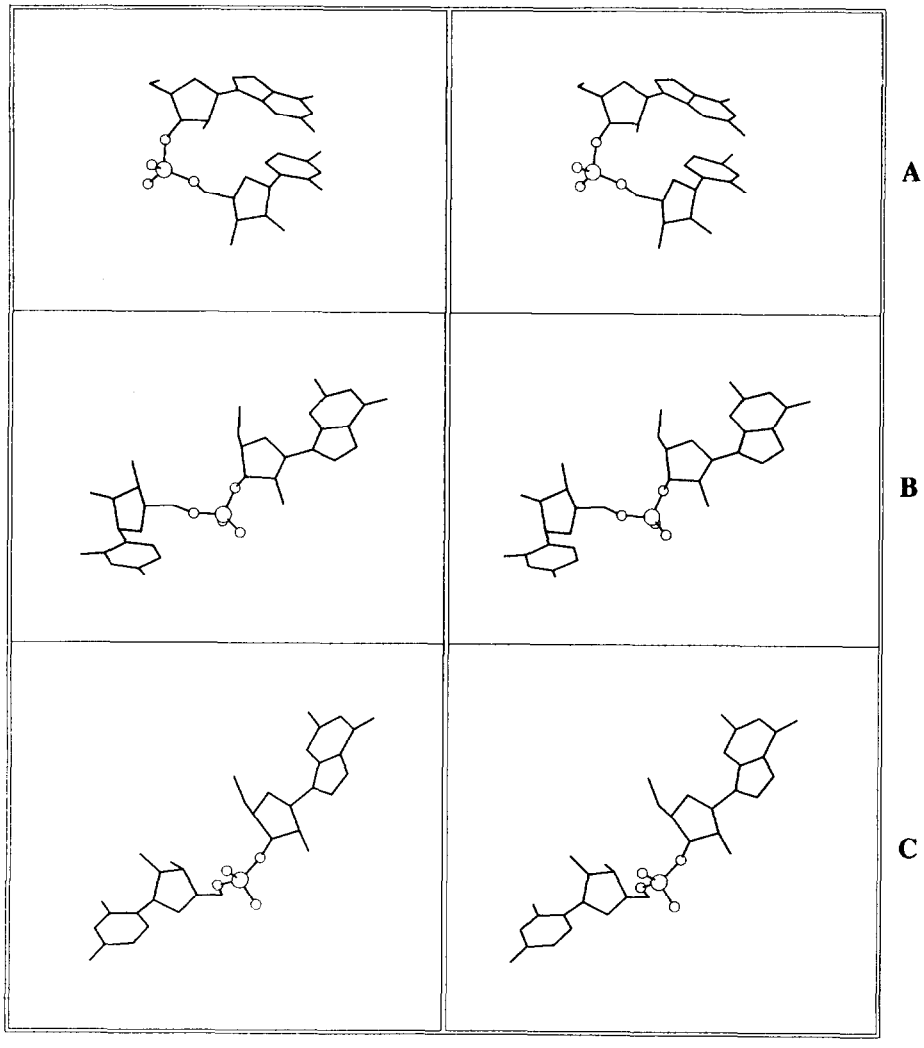

Figure 9: The stereoviews of conformation of the sugar-phosphate backbone at the self-cleavage site (G^3 and C^6 (in hexamer **1**) or U^7 (in heptamer **2**)) from the snapshots at 226 ps. All water molecules, sodium ions, and hydrogen atoms have been omitted for clarity. The O3'-PO_2-O5' fragments are shown as ball and stick models while the remainder is shown as wireframe. Panel (A): Hexamer **1** A-form (P of G^3 = 44°, ε = -158°, ζ = -58°, α = -80°, β = 171°, γ = 68° and P of C^6 = 53°). Panel (B): Hexamer **1** B-form (P of G^3 = 177°, ε = -151°, ζ = 78°, α = 85°, β = 178°, γ = 67° and P of C^6 = 37°). Panel (C): Heptamer **2** (P of G^3 = 123°, ε = -96°, ζ = 146°, α = 64°, β = -176°, γ = 54° and P of U^7 = 150°).

to a particular environment. This has been observed[42] in triple helices where cytosine is able to protonate the triple helice at neutral pH. Although the stabilization of the trigonal bipyramidal transition state will also contribute to an increase of cleavage rate. Thus, it has been shown that for the hairpin ribozyme (k_{cat} = 2 min^{-1}), a guanosine base at the 3'-end of the cleavage site is required for the catalysis[43], and molecular modelling have suggested that the 2-amino group of guanosine is well positioned to assist in phosphate cleavage[43]. The rate of self-cleavage of hexamer **1** and heptamer **2** was slow enough (k = 0.25 10^{-4} min^{-1} for **1**, k = 0.16 10^{-3} min^{-1} for **2**) to allow a full structure determination by NMR compared to the the self-cleavage of hammerhead ribozyme (k = 0.5 min^{-1}) . However, the absence of interresidual nOe's and of imino hydrogen bonding makes a full structure determination difficult. Especially, the identification of base-phosphate, base-sugar and sugar-phosphate interactions has not been possible. Several observations are however of strong interest:

(1) The ability to undergo self-cleavage and the rate of the self-cleavage reaction depends on the size of the loop. The heptamer **2** cleaves six times faster than the hexamer **1**, whereas a pentameric lariat with a loop of three nucleotides and a 3'-tail of two nucleotides does not self-cleave[9,50].

(2) The nucleotides of the 3'-tail, or some specific functional group(s) of the 3'-tail are necessary for the self-cleavage or are critical for the formation or stabilization of the transition state. Thus, the cyclic A(2'→5')G linked tetramer **3** does not self-cleave.

(3) The addition of Mg^{2+} increases the rate of cleavage, but it does not change the conformation of the ribose rings nor the conformation of the glycosidic bond. Probably, the coordination of Mg^{2+} to the non-bridging phosphate oxygens help self-cleavage by stabilizing the transition state, but it is not necessary for its formation.

(4) NMR and molecular modelling have shown that the loop nucleotides in heptamer **2** have ribose, glycosidic bond and phosphate backbone conformations that are very similar to those of the B-form of hexamer **1**. At low temperature, the conformation of the non-cleaving A(2'→5')G linked tetramer **3** is very similar to the conformation of the A-form of hexamer **1**.

(5) The pH dependence of the rate of the Lariat-RNA self-cleavage reaction, which peaks at pH 6, suggests an intramolecular base-acid catalyzed mechanism.

These results indicate that a certain conformational flexibility is necessary to reach or to switch to a conformation which is favourable for cleavage. Even if the ground state conformation determined by NMR and refined by molecular modelling is not the conformation of the intermediate or transition state required for the self-cleavage reaction, one can postulate that the transition state conformation is more easily reached from the the ground state conformation of the heptamer than from the ground state conformation of the hexamer. Some functional groups of the 3'-tail, possibly the N3 or the 4-amino group of cytidine, may assist the self-cleavage reaction by forming hydrogen bond or by being involved in proton transfer reactions.

Studies are now in progress to identify the important functional groups in the 3'-tail as well as to assess the implication of additional nucleotides in the loop on the overall conformation and rate of cleavage.

Experimental

*Synthesis of cyclic (2'→5') linked tetramer **3** , cyclic (3'→5') linked tetramer **4** and cyclic branched lariat hexamer **1***

^{1}H-NMR spectra were recorded in δ scale with Jeol FX 90 Q and Bruker AMX-500 spectrometers at 90 and 500 MHz respectively, using TMS or H_2O (set at 4.7 ppm) as internal standards. ^{31}P-NMR spectra were

recorded at 36 and 202 MHz in the same solvent using 85 % phosphoric acid as external standard. Thin layer chromatography was carried out using pre-coated Merck silica gel F_{254} TLC or HPTLC plates in the following CH_2Cl_2-MeOH mixtures: (A) 90: 10 (v/v), (B) 86: 14 (v/v), (C) 80: 20 (v/v). Dry pyridine was obtained by distillations from CaH_2 and TsCl. MeCN was distilled from P_2O_5 under argon. Dimethylformamide (DMF) was distilled from CaH_2. Et_3N and DBU was distilled from CaH_2 under argon. Column chromatography of all the protected intermediates wa carried out using Merck G 60 silica gel. DEAE-Sephadex A-25 from Pharmacia was used for the ion exchange chromatography. An LDC equipment with ConstaMetric Pump model III and Gradient Master was used for analytical HPLC chromatography. A Gilson equipment with Pump Model 303, Manometric Module Model 802C and Dynamic Mixer 811B connected to a Dynamax computer program for gradient control was used for semi-preparative RP-HPLC separations. 2'-O-Thp derivatives of all nucleosides used in this work were separated and used in a diastereomerically pure form which are designated as "Low R_f" or "High R_f" subsequently in the following experimental section. All reactions were carried out at RT (≈ 20°C), unless otherwise specified. Analytical HPLC and high pressure semi-preparative Spherisorb S50DS2 column chromatography were carried out using gradients of solution B (50 % MeCN in 0.1 M triethylammonium acetate (TEAA)) in solution A (5 % MeCN in 0.1 M TEAA).

Compound 11 : 6-N-anysoyl-3'-5'-O-(tetraisopropyl-1,3-disiloxane-1,3-dilyl) (TipdSi)-adenosine-2'-O-(2 chlorophenyl)(cyanoethyl)phosphate (619 mg, 0.7 mmol) was dissolved in dioxane (14 ml) and treated with 0.2 M aq. HCl (9.75 ml) resulting in an opalescent solution. A few drops of this 0.2 M aq. HCl solution were added frequently to keep the reaction mixture opalescent. After 50 min at RT the reaction was quenched by pouring into the saturated $NaHCO_3$ solution (50 ml) and extracted with CH_2Cl_2 (4 x 30 ml). The organic phase was dried and purified by silica gel chromatography to afford the desired 5'-hydroxy block **11** (500 mg, 79 %); R_f: 0.55 (A). ^{1}H-NMR ($CDCl_3$): 9.03 (br, 1H) NH; 8.74 (s, 1H) H-8; 8.16 (s, 1H) H-2; 8.04 (s, 1H) -CO*Ph*CH_3; 7.94 (s, 1H) -CO*Ph*CH_3; 7.17 (m, 4H) 2-Cl*Ph*; 7.03 (s, 1H) -CO*Ph*CH_3; 6.93 (s, 1H) -CO*Ph*CH_3; 6.25 (d, $J_{1'-2'}$ = 6.3 Hz, 1H) H-1'; 5.77 (m, 1H) H-2'; 5.05 (m, 1H) H-3'; 4.34-3.96 (m, 5H) H-4', H-5', H-5", -O*C*$H_2$$CH_2$CN; 3.88 (s, 3H) -COPhC*H*$_3$; 2.60 (t, 2H) -OCH_2*C*H_2CN; 1.05 (m, 28H) TipdSi. ^{31}P NMR ($CDCl_3$) -8.32 ppm.

Compound 12a : A mixture of **10b** (*Low Rf-Low Rf*) (500 mg, 0.29 mmol) and **11** (206 mg, 0.23 mmol) were dissolved in dry pyridine (2 ml). MSNT was added (280 mg, 0.95 mmol) and the reaction mixture stirred under argon for 75 min. An aqueous $NaHCO_3$ work-up, followed by silica gel chromatography (1-3 % EtOH / 0.5 % pyridine / CH_2Cl_2) afforded the trimer **12a** as a white powder after co-evaporation with toluene and cyclohexane respectively (440 mg, 77 %); R_f: 0.8 (A). ^{1}H-NMR ($CDCl_3$+CD_3OD+lutidine): 8.76 (s, 1H) AH-8; 8.36 (s, 1H) AH-2; 8.12-6.75 (m, 40H) arom, CH-6, CH-5, & UH-6; 6.40 (m, 2H) AH-1', UH-1'; 6.13-5.71 (m, 5H) AH-2', CH-1', CH-2', UH-2' & UH-5, 5.08-4.20 (m, 16H) sugar protons, 2 x Thp, -O*C*$H_2$$CH_2$CN; 3.88 (s, 9H) 3 x -COPh*C*H_3; 3.79 (s, 6H) 2 x OCH_3, 3.58-2.85 (m, 4H) 2 x Thp; 2.72 (t, 2H) -OCH_2*C*H_2CN; 1.48 (m, 12H) 2 x Thp; 1.05 (m, 28H) TipdSi. ^{31}P-NMR ($CDCl_3$+CD_3OD+lutidine): -6.90, -7.00 &-7.32 ppm.

Compound 12b : The trimer **12a** (*Low Rf - Low Rf*) (440 mg, 0.179 mmol) was dissolved in half of the calculated total volume of 2 % MeOH-CH_2Cl_2 solution and chilled to ~0 °C in an ice bath. Trichloroacetic acid (347 mg, 2.13 mmol) was dissolved in the second half of the 2 % MeOH-CH_2Cl_2 solution and chilled to ~0 °C prior to pouring into the above solution of **12a**. The final concentration of acid was 0.055 M · After stirring for 2h 30 min at ~0 °C the reaction was quenched by a small amount of pyridine, and then poured into 0.2 M NH_4HCO_3 solution which was saturated with NH_4Cl and acidified with dry ice. This aqueous phase (pH ~6.5) was extracted with CH_2Cl_2 (3 x 50 ml) and the organic phase obtained was concentrated and purified by column chromatography to give **12b** (257 mg, 66 %); R_f: 0.5 (A). ^{1}H-NMR ($CDCl_3$+CD_3OD): 8.71 (s, 1H) AH-8; 8.30-6.87 (m, 28H) arom, AH-2, CH-6, CH-5 & UH-6; 6.47-5.74 (m, 6H) AH-1', AH-2', CH-1', CH-2' & UH-1', UH-5 ; 5.22-4.10 (m, 16H) sugar protons, 2 x Thp, -O*C*$H_2$$CH_2$CN; 3.88 (s, 9H) -COPhC*H*$_3$; 3.50 (m, 4H) 2 x Thp; 2.80 (m, 2H) -OCH_2*C*H_2CN; 1.43 (m, 12H) 2 x Thp; 1.05 (m, 28H) TipdSi. ^{31}P-NMR ($CDCl_3$+CD_3OD): -6.83; -6.94; -7.12, -7.25 ppm.

Compound 14a : A mixture of **12b** (*Low Rf - Low Rf*) (257 mg, 0.118 mmol) and **13** (*LowRf*) (204 mg, 0.177 mmol) was co-evaporated with dry pyridine and redissolved in dry pyridine (1 ml). MSNT (243 mg, 0.82 mmol) was added and the reaction mixture was stirred for 4h 30 min. Aqueous NH_4HCO_3 work up followed by silica gel column chromatography (2-5 % EtOH in CH_2Cl_2) gave the fully protected tetramer **14a** as a white powder after co-evaporation with toluene and cyclohexane (330 mg, 84 %); R_f: 0.57(A). ^{1}H-NMR ($CDCl_3$+lutidine): 8.77 (s, 1H) AH-8; 8.57-6.80 (m, 54H) arom, AH-2, CH-6, CH-5, UH-6, GH-8; 6.65 (m, 1H) AH-1'; 6.43-5.11 (m, 10H) anomeric, sugar protons, UH-5; 4.71-4.08(m, 19H) sugar protons, 3 x Thp, -O*C*$H_2$$CH_2$CN; 3.86 (s, 9H) 3 x -COPhC*H*$_3$; 3.63 (s, 6H) 2 x OCH_3; 3.46-2.86 (m, 6H) 3 x Thp; 2.70 (m, 2H)

-OCH_2CH_2CN; 1.61 (m, 18H) 3 x Thp; 1.47 (s, 9H) *t-butyl*; 1.03 (m, 28H) TipdSi. ^{31}P-NMR ($CDCl_3$+CD_3OD+lutidine): -6.76; -6.88; -6.95; -7.10; -7.17 & -7.25 ppm.

Compound 14b : The tetramer **14a** (330 mg, 0.1 mmol) was detritylated using a similar condition as described for **12a**. After stirring for 4 h followed by an aq. NH_4HCO_3 work-up the organic phase was dried and purified by silica gel chromatography. The 5'-hydroxy-2'phosphodiester block **14b** was obtained as a white powder, after co-evaporation with toluene and cyclohexane (246 mg, 83 %); R_f: 0.6 (A). ^{1}H-NMR ($CDCl_3$): 8.73, 8.71 (2 x s, 1H) AH-8; 8.55-6.78 (m, 41H) arom, AH-2, GH-8, CH-5, CH-6, UH-6; 6.46-5.59 (m, 11H) anomeric, UH-5 & sugar protons; 4.92-4.16 (m,19H) sugar protons, 3 x Thp, -OCH_2CH_2CN; 3.88, 3.80 (2 x s, 9H) 3 x -$COPhCH_3$; 3.53-3.00 (m, 6H) 3 x Thp; 2.69 (m, 2H) -OCH_2CH_2CN; 1.43 (m, 18H) 3 x Thp; 1.31 (s, 9H) *t-butyl*; 1.02 (m, 28H) TipdSi. ^{31}P-NMR ($CDCl_3$ + CD_3OD): -7.17; -7.37; -7.66; -7:86 ppm.

Compound 14c : Compound **14b** (246 mg, 0.082 mmol) was co-evaporated in dry pyridine and redissolved in the same solvent (0.9 ml). To the mixture was added dry Et_3N (228 µl, 20 equiv) and the solution stirred for 3 h 30 min under argon atmosphere. After stirring the reaction was diluted with 25 ml of dry pyridine and transfered in a 50 ml flask and then finally evaporated till dryness. The residue was redissolved in dry CH_2Cl_2, diluted with dry toluene and evaporated. Silica gel chromatography afforded **14c** (Et_3NH^+ salt, 247 mg, 98 %); R_f: 0.6 (B). ^{1}H-NMR ($CDCl_3$): 8.65 (s, 1H) AH-8; 8.41-6.80 (m, 41H) arom, AH-2; GH-8; CH-6; CH-5; UH-6; 6.38-4.84 (m, 11H) UH-5, anomeric & sugar protons; 4.83-4.04 (m, 17H) sugar protons , 3 x Thp; 3.87, 3.86 (2 x s , 9H) 3 x -$COPhCH_3$; 3.71-3.17 (m, 6H) 3 x Thp; 1.46 (m, 18H) 3 x Thp; 1.30 (s, 9H) *t-butyl* ; 1.05 (m, 28H) TipdSi. ^{31}P-NMR ($CDCl_3$): [-6.76, -6.86] and [-7.42; -8.15] ppm.

Fully protected tetrameric cyclic RNA 15 : The 5'-hydroxy-2'-phosphodiester block **14c** (247 mg, 0.08 mmol) was co-evaporated with dry pyridine and redissolved in dry pyridine (250 ml / mmol, 4 mM). Then MSNT (484 mg, 24 eq) was added to the reaction solution over a period of 36 h. Aqueous NH_4HCO_3 work up followed by silica gel column chromatography (2-5 % EtOH in CH_2Cl_2) afforded the title compound **15** as a white powder after co-evaporation with toluene and cyclohexane (80 mg, 33 %); R_f: 0.9 (A). ^{1}H-NMR ($CDCl_3$ + CD_3OD): 8.65 (s, 1H) AH-8; 8.80-6.80 (m, 41H) arom, AH-2, GH-8, CH-6, CH-5, UH-6; 6.20-5.05 (m, 11H) UH-5, anomeric & sugar protons; 5.00-4.00 (m, 17H) sugar protons, 3 x Thp ; 3.87 (m, 9H) 3 x -$COPhCH_3$; 3.5-2.7 (m, 6H) 3 x Thp ; 1.60 (m, 18H) Thp; 1.30 (m, 9H) *t-butyl*; 1.05 (m, 28H) TipdSi. ^{31}P-NMR ($CDCl_3$+CD_3OD): -7.21 to -8.17 ppm (16 peaks).

Compound 17a : A mixture of **16** (*High Rf-High Rf*) (120 mg, 0.063 mmol) and **10c** (*High Rf-High Rf*) (102 mg, 0.075 mmol) was co-evaporated with dry pyridine and redissolved in dry pyridine (0.7 ml). MSNT (55 mg, 0.19 mmol) was added and the reaction mixture was stirred under argon for 2 h. An aq. NH_4HCO_3 work up followed by silica gel chromatography (1-3% EtOH / 0.5% pyridine / CH_2Cl_2) gave the fully protected tetramer **17a** as a white powder after co-evaporation with toluene and cyclohexane (161 mg, 81 %); R_f: 0.73 (A). ^{1}H-NMR ($CDCl_3$+lutidine): 8.63 (s, 1H) AH-8; 8.25-6.69 (m, 54H) arom, AH-2, GH-8, CH-6, CH-5 & UH-6; 6.43-5.52 (m, 6H) anomeric and sugar protons; 5.49-4.23 (m, 23H) UH-5, sugar protons, 4 x Thp & -OCH_2CH_2CN; 3.89, 3.86 (2 x s, 9H) 3 x -$COPhOCH_3$; 3.72 (s, 6H) 2 x -OCH_3 ; 3.88-3.65 (m, 2H) sugar protons; 3.51-2.81 (m, 8H) 4 x Thp; 2.36-2.21 (m, 2H) -OCH_2CH_2CN; 1.59 (m, 24H) 4 x Thp; 1.29 (s, 9H) *t-butyl*.. ^{31}P-NMR ($CDCl_3$+lutidine): -7.51, -7.66, -8.05, -8.10, -8.25 & -8.30 ppm.

Compound 17b : 5'-O-Dmtr-tetramer block **17a** (*all High Rf isomer*) (240 mg, 0.076 mmol) was dissolved in half of the calculated total volume of 2 % MeOH-CH_2Cl_2 solution and chilled to ~0 °C in an ice bath. Trichloroacetic acid (148 mg, 0.908 mmol) was dissolved in the second half of the 2 % MeOH-CH_2Cl_2 solution and chilled to ~0 °C prior to pouring it into the tetramer solution. The final concentration of acid was 0.055 M. After stirring for 4 h the reaction was quenched by a small amount of pyridine and then it was subjected to an aq. NH_4HCO_3 work up. Silica gel chromatography (2-5 % EtOH in CH_2Cl_2) afforded **17b** (169 mg, 78 %); R_f: 0.51 (A). ^{1}H-NMR($CDCl_3$): 9.10 (br, 1H) NH; 8.75 (s, 1H) AH-8; 8.31-6.78 (m, 41H) arom, AH-2, GH-8, CH-6, CH-5 & UH-6; 6.28-5.74 (m, 5H) anomeric and sugar protons; 5.72-4.40 (m, 24H) UH-5, sugar protons, 4 x Thp & -OCH_2CH_2CN; 4.01-3.68 (m, 2H) sugar protons; 3.85 (s, 9H) 3 x -$COPhOCH_3$; 3.59-3.06 (m, 8H) 4 x Thp; 2.89-2.76 (m, 2H) -OCH_2CH_2CN; 1.53 (m, 24H) 4 x Thp; 1.31 (s, 9H) *t-butyl*. ^{31}P-NMR ($CDCl_3$): -6.51, -6.83, -7.00, -7.07, -7.20, -7.29, -7.49 & -7.54 ppm.

Compound 17c : Compound **17b** (140 mg, 49 mmol) was treated with dry Et_3N (136 ml, 20 equiv) in dry pyridine (0.55 ml) and stirred for 3 h. The reaction mixture was diluted with dry pyridine and evaporated and then co-evaporated with toluene. Silica gel chromatography (8-10 % EtOH / CH_2Cl_2) afforded **17c** as a white powder after co-evaporation with toluene and cyclohexane. The tetramer **17c** was then dissolved in minimum amount of CH_2Cl_2 and added dropwise to a falcon tube containing 30 ml of cyclohexane. After centrifugation, the supernatant was decanted and the white powder dried overnight to give pure **17c**: (Et_3NH^+ salt, 98 mg, 71 %). R_f: 0.25 (A). ^{1}H-NMR ($CDCl_3$): 9.32 (br, 1H) NH; 8.76 (s, 1H) AH-8; 8.27 (s, 1H) AH-2; 8.11-6.78 (m, 40H) arom, GH-8, CH-6, CH-5 & UH-6; 6.22-5.61 (m, 6H) anomeric protons; 5.38-4.11 (m,

23H) UH-5, sugar protons & 4 x Thp; 3.87, 3.85 (2 x s, 9H) -COPh*CH3*; 3.81-3.22 (m, 8H) 4 x Thp; 1.53 (m, 24H) 4 x Thp; 1.30 (s, 9H) *t-butyl.* ^{31}P-NMR ($CDCl_3$): -6.20, -7.05, -7.49, -7.62, -7.83, -7.98 & -8.06 ppm.

Fully protected tetrameric cyclic RNA 18 : The 5'-hydroxy-3'-phosphodiester block **17c** (101 mg, 34.3 mmol) was co-evaporated with dry pyridine and redissolved in dry pyridine (250 ml / mmol, 4 mM). Then MSNT (101 mg, 0.34 mmol) was added to the reaction solution and was then stirred for 14 h. Aqueous NH_4HCO_3 work up followed by silica gel column chromatography (2-4 % EtOH in CH_2Cl_2) afforded **18** as white a powder after co-evaporation with toluene and cyclohexane: (85 mg, 85 %); R_f: 0.72 (A). ^{1}H-NMR ($CDCl_3$ +CD_3OD): 8.76 (s, 1H) AH-8; 8.46-6.81(m, 41H) arom, AH-2, GH-8, CH-6, CH-5, UH-6; 6.23-4.92 (m, 12H) UH-5, anomeric & sugar protons; 4.91-4.35 (m, 17H) sugar protons & 4 x Thp; 3.85 (3 x s, 9H) 3 x COPh*CH3*; 3.50-2.85 (m, 8H) 4 x Thp; 1.64 (m, 24H) 4 x Thp; 1.28 (s, 9H) *t-butyl.* ^{31}P-NMR ($CDCl_3$+CD_3OD): -6.52 to -8.75 ppm (16 lines).

Compound 20a : The 3'-phosphodiester block **10a***(High Rf - High Rf)* (1.70 g, 1.25 mmol) was condensed with 6-N-benzoyl-2'-O-pixyladenosine **19** (1.10 g, 1.75 mmol) in dry pyridine (18 ml) by addition of 1-mesitylene-3-nitro-1,2,4-triazole (MSNT) (1.65 g, 5.58 mmol). The reaction mixture was then stirred for 60 min. Aqueous NH_4HCO_3 work up followed by silica gel column chromatography (using the silica gel pre-washed with 1 % Et_3N - CH_2Cl_2 mixture followed by washing with pure CH_2Cl_2) with 0-4 % EtOH/0.5 % pyridine in CH_2Cl_2 afforded **20a** as a white powder after co-evaporation with toluene and cyclohexane (1.61 g, 0.825 mmol, 66 %); R_f: 0.70 (A). ^{1}H-NMR ($CDCl_3$+lutidine): 9.11 (br, 1H) NH; 8.58-8.53 (m, 1H) AH-8; 8.25-6.23 (m, 39H) arom, AH-2, CH-6, CH-5 & UH-6; 6.05-5.67 (m, 4H) CH-1', UH-1', AH-1' & UH-5; 5.14-4.14 (m, 16H) sugar protons & 2 x Thp; 3.91-3.17 (m, 5H) 2 x Thp & AH-3'; 2.68 (m, 4H) -CO*CH2CH2*COCH3; 2.40 (s, 3H) -COPh*CH3*; 2.19, 2.16 (2 x s, 3H) -COCH2CH2CO*CH3*; 1.58 (m, 12H) 2 x Thp. ^{31}P-NMR ($CDCl_3$+lutidine): -7.10, -7.25, -7.78, -7.86, -7.93, -8.06 ppm.

Compound 20b : Compound **20a** *(High Rf - High Rf)* (1.61 g, 0.825 mmol) in dry pyridine (8 ml) was treated with 0.2 M MeCN solution of *o*-chlorophenylphosphoro-bis-(1,2,4-triazolide) (12.4 ml, 2.48 mmol) for 40 min. Aqueous NH_4HCO_3 work up followed by silica gel column chromatography (using the silica gel pre-washed with 1 % Et_3N - CH_2Cl_2 mixture followed by washing with pure CH_2Cl_2) with 0-7 % EtOH/1 % pyridine in CH_2Cl_2 afforded **20b** as a white powder after co-evaporation with toluene and cyclohexane (NH_4^+ salt, 1.68 g, 0.778 mmol, 94 %); R_f: 0.74 (C). ^{1}H-NMR ($CDCl_3$+CD_3OD+lutidine): 8.62, 8.53 (2 x s, 1H) AH-8; 8.26-5.75 (m, 47H) arom, AH-2, CH-6, CH-5 & UH-6, AH-1', UH-1', CH-1', & UH-5; 5.17-4.10 (m, 16H) sugar protons & 2 x Thp; 3.55 (m, 4H) 2 x Thp; 2.68 (m, 4H) -CO*CH2CH2*COCH3; 2.40 (s, 3H) -COPh*CH3*; 2.17 (s, 3H) -COCH2CH2CO*CH3*; 1.60 (m, 12H) 2 x Thp. ^{31}P-NMR($CDCl_3$+CD_3OD+lutidine): -7.59 to -8.42 ppm.

Compound 20c : The 3'-phosphodiester block **20b** *(High Rf - High Rf)* (1.68 g, 0.778 mmol) was dissolved in half of the calculated total volume of 2 % MeOH-CH_2Cl_2 solution and chilled to ~0 °C in an ice bath. Trichloroacetic acid (1.27 g, 7.78 mmol) was dissolved in the second half of the 2 % MeOH-CH_2Cl_2 solution and chilled to ~0 °C prior to addition into the above solution of **20b**. The final concentration of acid was 0.055 M. After stirring for 60 min at ~0 °C, the solution was poured into 0.2 M NH_4HCO_3 solution which was saturated with NH_4Cl and acidified with dry ice. This aqueous phase (pH ~6.5) was then extracted with CH_2Cl_2 (3 x 50 ml). The organic phase obtained was dried in $MgSO_4$ and filtered and evaporated. The residue was dissolved in a small amount of CH_2Cl_2 and pipetted into a diethylether-hexane solution (150 ml) (2:1 v/v). The precipitate was centrifuged, the supernatant was decanted and the white pixyl-free solid **20c** was dried *in vacuo* (NH_4^+ salt, 1.13 g, 0.596 mmol, 77 %); R_f: 0.65 (C). ^{1}H-NMR ($CDCl_3$+CD_3OD): 8.72 (s, 1H) AH-8; 8.39-6.85 (m, 30H) arom, AH-2, CH-6, CH-5 & UH-6; 6.21-5.90 (m, 3H) AH-1', CH-1' & UH-1'; 5.79, 5.76 (2 x d, J = 7.78Hz, 8.55Hz, 1H) UH-5; 5.22-4.13 (m, 16H) sugar protons & 2 x Thp; 3.50 (m, 4H) 2 x Thp; 2.41 (s, 3H) -COPh*C H3*; 2.68 (m, 4H) -CO*C H2CH2*COCH3; 2.19, 2.16 (2 x s, 3H) -COCH2CH2CO*CH3*; 1.55 (m, 12H) 2 x Thp. ^{31}P-NMR ($CDCl_3$+CD_3OD): -7.25 to -8.32 ppm.

Compound 20d : Bis(2-cyanoethoxy)-(diisopropylamino)phosphine (1.56 g, 5.77 mmol) was weighed into a dry 100 ml RB flask and dry 15 % DMF/ MeCN solution (19 ml) was added under argon. Then dry and sublimed tetrazole (1.21 g, 17.3 mmol) was added with stirring, and it rapidly went into solution followed by a quick formation of a precipitate. After 3 min stirring, solid 2'-hydroxy-3'-phosphodiester block **20c** *(High Rf - High Rf)* (1.10 g, 0.58 mmol) was added to the suspension and the resulting clear solution was then stirred for 40 min at RT under argon. A solution of 0.1 M I_2 / THF / pyridine / H_2O (7:2:1 v/v/v) (61 ml) was added. The resulting solution was stirred for 15 min, poured into 0.1 M $Na_2S_2O_3$ / concentrated NH_4HCO_3 solution (75 ml) and extracted with CH_2Cl_2 (3 x 75 ml). The pyridine-free gum obtained after toluene co-evaporation of the organic residue was then purified by short silica gel column chromatography (2-8 % EtOH in CH_2Cl_2) to finally give the 3'-phosphodiester-2'-bis(2-cyanoethoxy)phosphotriester block **20d** as a white powder after co-evaporation with toluene and cyclohexane (NH_4^+salt, 599 mg, 50 %); R_f: 0.69 (C). ^{1}H-NMR

($CDCl_3$+CD_3OD): 8.69, 8.66 (2 x s, 1H) AH-8; 8.35-6.84 (m, 30H) arom, AH-2, CH-6, CH-5 & UH-6; 6.33 (m, 1H) AH-1'; 6.10-5.65 (m, 5H) AH-1', CH-1', UH-1', UH-5 & AH-2'; 5.44 (m, 1H) AH-3'; 5.13-4.14 (m, 20H) sugar protons, 2 x Thp, 2 x -O*CH*$_2$$CH_2CN$; 3.50 (m, 4H) 2 x Thp; 2.90-2.47 (m, 8H) 2 x -OCH_2*CH*$_2$CN & -CO*CH*$_2$*CH*$_2$$COCH_3$; 2.41 (s, 3H) -COPh*CH*$_3$; 2.19, 2.16 (2 x s, 3H) -$COCH_2CH_2CO$*CH*$_3$; 1.45 (m, 12H) 2 x Thp. ^{31}P-NMR ($CDCl_3$+CD_3OD): -5.02, [-7.37 to -8.72] ppm.

Compound 22a : A mixture of **20d** *(High Rf - High Rf)* (599 mg, 0.288 mmol) and **21***(LowRf)* (490 mg, 0.432 mmol) was co-evaporated with dry pyridine and redissolved in dry pyridine (1.5 ml). MSNT (597 mg, 2.02 mmol) was added and the reaction mixture was stirred for 6 h. Aqueous NH_4HCO_3 work up followed by silica gel column chromatography (2-5 % EtOH in CH_2Cl_2) gave the fully protected pentamer **22a** as a white powder after co-evaporation with toluene and cyclohexane (492 mg, 54 %); R_f: 0.55 (A). ^{1}H-NMR ($CDCl_3$): 9.21 (br, 1H) NH; 8.74 (s, 1H) AH-8; 8.33-6.93 (m, 46H) arom, AH-2, 2 x CH-6, 2 x CH-5 & 2 x UH-6; 6.47 (m, 1H) AH-1'; 6.15-5.41 (m, 11H) 2 x CH-1', 2 x UH-1', 2 x UH-5, AH-2', 3', CH-2', 3' & UH-3'; 5.12-4.03 (m, 26H) sugar protons, 3 x Thp & 2 x -O*CH*$_2$$CH_2CN$; 3.50 (m, 6H) 3 x Thp; 2.81-2.49 (m, 8H) 2 x -OCH_2*CH*$_2$CN & -CO*CH*$_2$*CH*$_2$$COCH_3$; 2.40 (s, 3H) -COPh*CH*$_3$; 2.16 (s, 3H) -$COCH_2CH_2CO$*CH*$_3$; 2.06, 2.04 (2x s, 6H) 2 x -$COCH_3$; 1.48 (m, 18H) 3 x Thp. ^{31}P-NMR ($CDCl_3$+CD_3OD): [-3.22 to -3.68] & [-6.74 to -8.81] ppm.

Compound 22b : The pentamer **22a** (492 mg, 0.154 mmol) was dissolved in dry pyridine (2 ml). Then 0.5 M NH_2NH_2 hydrate (10 equiv) in pyridine/AcOH (3:2 v/v) (3.08 ml) was added to the reaction mixture and after 5 min stirring, the reaction was quenched by addition of pentane-2,4-dione (150 µl, 1.54 mmol, 10 equiv). The reaction mixture was then subjected to aqueous NH_4HCO_3 work up. The pyridine-free gum obtained after evaporation and co-evaporation with toluene was then purified by silica gel chromatography (2-4 % EtOH in CH_2Cl_2) to give **22b** as a white powder after co-evaporation with toluene and cyclohexane: (346 mg, 73 %); R_f: 0.49 (A). ^{1}H-NMR ($CDCl_3$+CD_3OD): 8.74 (s, 1H) AH-8; 8.52-6.90 (m, 46H) arom, AH-2, 2 x CH-6, 2 x CH-5 & 2 x UH-6; 6.45 (m, 1H) AH-1'; 6.11-5.63 (m, 11H) 2 x UH-5, anomeric & sugar protons; 5.42-4.05 (m, 26H) sugar protons, 3 x Thp & 2 x -O*CH*$_2$$CH_2CN$; 3.97-3.28 (m, 8H) CH-5', 5" & 3 x Thp; 2.65 (m, 4H) 2 x -OCH_2*CH*$_2$CN; 2.41 (s, 3H) -COPh*CH*$_3$; 2.08, 2.05 (2 x s, 6H) 2 x -$COCH_3$; 1.47 (m, 18H) 3 x Thp. ^{31}P-NMR ($CDCl_3$+CD_3OD): [-3.22 to -3.47] & [-6.93 to -8.32] ppm.

Compound 24a : 5'-O-(4,4'-dimethoxytrityl)- 2'-O-tetrahydropyranyl- 2-N-(*t*-butylbenzoyl)- 6-O-(2-nitro phenyl) guanosine-3'-triethylammonium (2-chlorophenyl)phosphate **23** *(Low Rf)* (174 mg, 0.168 mmol) and **22b** *(High-High-Low Rf)* (346 mg, 0.115 mmol) were co-evaporated with dry pyridine and redissolved in dry pyridine (0.5 ml). (MSNT) (150 mg, 0.504 mmol) was added and the reaction mixture was stirred for 3 h. Aqueous NH_4HCO_3 work up followed by silica gel column chromatography of the organic residue (0-5 % EtOH-CH_2Cl_2) gave the fully protected oligomer **24a** *(Low-High-High-Low Rf)* as a white powder after co-evaporation with toluene and cyclohexane (403 mg, 0.103 mmol, 90 %); R_f: 0.53 (A). ^{1}H-NMR ($CDCl_3$): 9.26 (br, 1H) NH; 8.70 (m, 1H) AH-8; 8.49-6.97 (m, 55H) arom, AH-2, GH-8, 2 x CH-6, 2 x CH-5 & 2 x UH-6; 6.46 (m, 1H) AH-1'; 6.22-5.43 (m, 14H) 2 x UH-5, anomeric & sugar protons; 5.25-4.01 (m, 32H) sugar protons, 4x Thp, 2 x -O*CH*$_2$$CH_2CN$; 3.49 (m, 8H) 4 x Thp; 2.72-2.49 (m, 8H) 2 x -OCH_2*CH*$_2$CN, -CO*CH*$_2$*CH*$_2$$COCH_3$; 2.40 (s, 3H) -COPh*CH*$_3$; 2.06, 2.03 (2 x s, 9H) -$COCH_2CH_2CO$*CH*$_3$, 2 x -$COCH_3$; 1.46 (m, 24H) Thp; 1.30 (s, 9H) *t-butyl.* ^{31}P-NMR ($CDCl_3$+CD_3OD): [-3.25 to -3.54] & [-6.69 to -9.01] ppm.

Compound 24b : The fully protected oligomer **24a** (403 mg, 0.103 mmol) was dissolved in dry pyridine (1.5 ml). Then 0.5 M NH_2NH_2 hydrate (10 equiv) in pyridine/AcOH (3:2 v/v) (2.06 ml) was added to the reaction mixture and after 5 min stirring, the reaction was quenched by addition of pentane-2,4-dione (100 µl, 1.03 mmol, 10 equiv). The reaction mixture was then subjected to aq. NH_4HCO_3 work up. The pyridine-free gum obtained after evaporation and co-evaporation with toluene was then purified by silica gel chromatography (3-5 % EtOH in CH_2Cl_2) to give **24b** as a white powder after co-evaporation with toluene and cyclohexane (259 mg, 66 %); R_f: 0.49 (A). ^{1}H-NMR ($CDCl_3$): 9.46 (br, 1H) NH; 8.70 (m, 1H) AH-8; 8.37-6.94 (m, 55H) arom, AH-2, GH-8, 2 x CH-6, 2 x CH-5 & 2 x UH-6; 6.46 (m, 1H) AH-1'; 6.25-5.45 (m, 14H) 2 x UH-5, anomeric & sugar protons; 5.26-4.00 (m, 30H) sugar protons, 4 x Thp & 2 x -O*CH*$_2$$CH_2CN$; 3.78-3.26 (m, 10H) GH-5', 5" & 4 x Thp; 2.61 (m, 4H) 2 x -OCH_2*CH*$_2$CN; 2.39 (s, 3H) -COPh*CH*$_3$; 2.06, 2.05 (2 x s, 6H) 2 x -$COCH_3$; 1.46 (m, 24H) 4 x Thp; 1.31 (s, 9H) *t-butyl.* ^{31}P-NMR ($CDCl_3$+CD_3OD): -3.22, -3.39, -3.51 & [-6.73 to -8.81] ppm.

Compound 24c : The hexamer **24b** (259 mg, 0.068 mmol) was treated with dry diisopropylethylamine (297 µl, 1.71 mmol, 25 equiv, 30 % concentration in dry pyridine, 0.55 ml) and stirred for 1 h at 40 °C. The reaction mixture was diluted with dry pyridine and evaporated and then co-evaporated with toluene and the pyridine free residue was purified by silica gel chromatography (3-8 % EtOH in CH_2Cl_2) to give **24c** as a white powder after co-evaporation with toluene and cyclohexane (177 mg, 67%); R_f: 0.28 (A). ^{1}H-NMR ($CDCl_3$ +CD_3OD): 8.71 (m, 1H) AH-8; 8.47-6.95 (m, 55H) arom, AH-2, GH-8, 2 x CH-6, 2 x CH-5 & 2 x

UH-6; 6.36 (m, 1H) AH-1'; 6.25-5.40 (m, 14H) 2 x UH-5, anomeric & sugar protons; 5.25-4.19 (m, 28H) sugar protons, 4 x Thp & -OCH_2CH_2CN; 3.98 -3.27 (m, 10H) GH-5', 5" & 4 x Thp; 2.60 (m, 2H) -OCH$_2$CH_2CN; 2.39 (s, 3H) -COPhCH_3; 2.04, 2.02 (2 x s, 6H) 2 x -COCH$_3$; 1.48 (m, 24H) 4 x Thp; 1.30 (s, 9H) *t-butyl*. ^{31}P-NMR ($CDCl_3$+CD_3OD): -1.29, -1.53 & [-7.13 to -8.23] ppm.

Fully protected hexameric lariat RNA 25 : The 5'-hydroxy 3'-phosphodiester block **24c** (177 mg, 0.046 mmol) was co-evaporated with dry pyridine and redissolved in dry pyridine (11.5 ml, 4 mM of **24c**). Then MSNT (123 mg, 0.414 mmol) was added to the reaction solution and was then stirred for 15 h. Aqueous NH_4HCO_3 work up followed by silica gel column chromatography (2-5 % EtOH in CH_2Cl_2) afforded the title compound **25** as white a powder after co-evaporation with toluene and cyclohexane: (122 mg, 72 %); R_f: 0.44 (A). ^{1}H-NMR ($CDCl_3$ +CD_3OD): 8.78-6.96 (m, 52H) arom, AH-8, AH-2, GH-8, 2 x CH-6, 2 x CH-5 & 2 x UH-6; 6.20-5.40 (m, 15H) 2 x UH-5, anomeric & sugar protons; 4.90-4.15 (m, 32H) sugar protons, 4 x Thp & -OCH_2CH_2CN; 3.57 (m, 8H) 4 x Thp; 2.62 (m, 2H) -OCH$_2$CH_2CN; 2.40 (s, 3H) -COPhCH_3; 2.06 (s, 6H) 2 x -COCH$_3$; 1.45 (m, 24H) 4 x Thp; 1.28 (s, 9H) *t-butyl*. ^{31}P-NMR ($CDCl_3$+CD_3OD): -0.63, [-1.83 to -4.90] & [-6.95 to -8.79] ppm.

Deprotections of 15 to 3, 18 to 4 and 25 to 1: Fully protected oligomers **15** (80 mg, 27.2 μmol), **18** (85 mg, 30.2 mmol) and **25** (89 mg, 23.9 μmol) were co-evaporated with distilled dioxane and dissolved in dioxane / water (8:2 v/v) solution (for **15**: 8.7 ml; for **18**: 9.2 ml; for **25**: 7 ml), *syn*-4-nitrobenzaldoxime (for **15**: 181 mg, 1.09 mmol; for **18**: 200 mg, 1.2 mmol; for **25**: 278 mg, 1.67 mmol) and 1,1,3,3-tetramethylguanidine (for **15**: 122 μl, 0.97 mmol; for **18**: 136 μl, 1.09 mmol; for **25**: 187 μl, 1.50 mmol) were then added[39,40]. After stirring for 40 h at RT the solvents were removed by evaporation *in vacuo* and concentrated ammonia (45 ml, d = 0.9) was added. The reaction mixture was stirred for 7 days at RT and was then evaporated and co-evaporated with distilled water. The residue was treated with 80% aq. acetic acid (35 ml) for 24 h at RT. After evaporation and co-evaporation with distilled water the residue was dissolved in distilled water (20 ml) and extracted with diethylether (3 x 20 ml) and subsequently with CH_2Cl_2 (6 x 20 ml) and the aqueous phase was evaporated to dryness. An additional deprotection step was applied in case of tetramer **15** to remove the TipdSi protecting group; the compound was dissolved in a minimum amount of water (350 μl) and THF (135 μl) was added. To this mixture a 1 M solution of TBAF/THF (0.95 ml, 5 equiv) was added and stirred for 1 h. The solution was evaporated to remove THF and co-evaporated with MeCN.

Purifications of 1, 3, and 4 : DEAE-Sephadex A-25 column chromatography was carried out by redissolving the residue in 0.001 M NH_4HCO_3 (BDH Chemicals Ltd, Poole, England) buffer and applied to a DEAE-Sephadex A-25 column (2 x 25 cm, HCO_3^- form) and eluted with a linear gradients 0.001 M - 0.25 M - 0.75 M in case of **3** and **4** and 0.001 M - 0.5 M - 0.8 M in case of **1**, of NH_4HCO_3 solution (500 ml/1000 ml/500 ml respectively; pH 7.5). The main symmetrical peak eluted between, 0.5 and 0.6 M in case of **3** and **4** and 0.7 and 0.8 M in case of **1** was collected (**3:** 420 A_{260} units, 40 %; **4:** 482 A_{260} units, 39 %; **1:** 712 A_{260} units, 52 %). Analytical HPLC (0-40 % solution B / solution A in 30 min, 1 ml / min) revealed that this material contained about 75-80 % of product. The product from the Sephadex was purified by high pressure semi-preparative Spherisorb S5ODS2 column chromatography. Batches of 5-7 mg of lyophilized material obtained from the middle- and rear fractions were each dissolved in solution A at pH 7.0 (900-1000 μl). These were taken in Eppendorf tubes, centrifuged and were then injected onto a semi-preparative Spherisorb S5ODS2 column (8 x 250 mm) equilibrated in solution A. Gradient elution with MeCN in 0.1M TEAA (0-5% solution B in 20 min, 1 ml/min) resolved the desired peak with base-line separation (detector was set at 254 nm). The purified material was collected, evaporated and then lyophilized several times (~9 x 1 ml) until the TEAA salt was removed (monitored by ^{1}H-NMR) to give **3** (Et_3NH^+ salt, 11 mg, 24 %), **4** (Et_3NH^+ salt, 16 mg, 31 %) and **1** (16.7 mg, 28 %). For preparation of NMR samples, the Et_3NH^+ salts of **1**, **3** and **4** were converted to the corresponding Na^+ salts by elution of appropriately sized batches with distilled water through a cooled Dowex column (1 x 20 cm, Na^+ form) at 2 °C. The eluted water was collected in a 50 ml round bottomed flask which was cooled in EtOH / dry ice bath. The frozen aqueous solution was lyophilized and the white residue was redissolved in a small amount of distilled water, swiftly transferred to a dry ice freezed 10 ml screw cap bottle and lyophilized and thereafter stored as a dry white solid.

Hplc measurements: The Hplc elution profiles of the self-cleavage reaction of hexamer **1** to give the cleaved hexamer **5** were run under the following condition: Gradient elution with 100 % buffer A to 40 % buffer B in 30 min, flow rate: 1 ml / min. Buffer A = 5 % MeCN in 0.1 triethylammonium acetate (TEAA), pH 7.0, Buffer B = 50 % MeCN in 0.1 M TEAA, pH = 7.0. **1** eluted at R_t = 9.40 min and **5** eluted at R_t = 10.50 min.

NMR spectroscopy: The NMR samples were lyophilized from 99.8% ^2H_2O, dissolved in 0.5 ml of 99.9% ^2H_2O and transferred into 5 mm tubes. The sample concentration used for recording the NMR spectra were as follows: hexamer **1**: 8 mM for 2D experiments, 2 mM for one dimensional ^{1}H- and ^{31}P-NMR,

kinetics and thermodynamic measurements. Following sample concentrations were used: 4.0 mM for heptamer **2**: 4.0 mM for tetramer **3** and tetramer **4**. All NMR spectra were recorded on a Bruker AMX-500 spectrometer operating at 500.13 MHz for proton, 202.4 MHz for phosphorus and 125.76 MHz for carbon. ^{1}H-NMR spectra were collected with 32K data points and zero filled to 64K. A trace of dry acetonitrile was added as an internal reference (set at 2.00 ppm) for ^{1}H-NMR chemical shifts measurements. ^{31}P-NMR spectra were acquired with 16K data points and zero filled to 32K. 3',5'-cyclic AMP was used as an external reference set at 0.00 ppm. The two-dimensional spectra were recorded in pure-phase absorption mode with the time proportional incrementation method and with low power preirradiation of the residual HDO peak during the relaxation delay. The DQF-COSY with and without ^{31}P decoupling were acquired with 8192 complex data points in t_2 and 512 points in t_1. The data were zero filled to give a 4096 x 2048 point matrix, and a $\pi/4$ shifted sine-square bell window was applied in both directions before Fourier transformation. For each crosspeak, the corresponding row was extracted as a 1D spectrum, backtransformed and zero filled twice before Fourier transformation. The final digital resolution was 0.25 Hz/pt. The clean-TOCSY spectra were acquired with 512 spectra of 4K data points using a sweep width of 4300 Hz. The t_1 domain was zero filled to 1K and a $\pi/2$ shifted sinesquare window was applied in both dimensions before Fourier transformation. The MLEV-17 sequence was applied for mixing using an extra delay of 65 μs for compensation of nOe, total mixing time 300ms. Two different power levels were used for excitation and spinlock. The NOESY and ROESY spectra were acquired with 2048 complex data points in t_2 and 256 points in t_1. The data were zero filled to give a 2048 x 1024 point matrix, and a sine-square bell window was applied in both directions before Fourier transformation. For ROESY, a CW spinlock (2.5 kHz) was used for mixing. Mixing times of 80, 100, 150 and 500 ms were used. The ^{1}H-^{31}P correlation experiments were run in the absolute value mode. A delay of 83 ms was used. 256 experiments were recorded, for each experiment we recorded 32 scans of 2K data points. The spectral range used was 1500 Hz in the t_1 direction and 4200 Hz in t_2. The spectrum was zero filled to 512 data points in t_1 and a sinesquare ($\pi/2$) window was applied before Fourier transformation. The ^{1}H-^{13}C chemical shift correlation experiments (HSQC) were recorded with 1200 experiments of 2048 points and 32 scans. Heteronuclear decoupling was achieved by the GARP-1 sequence. The spectral width was 4200 Hz in the ^{1}H direction and 2515 Hz in the ^{13}C dimension. The digital resolution was 1.0 Hz/point in the t_2 direction and 0.5 Hz/point in the t_1 direction.

Acknowledgements. Authors thank Swedish Board for Technical Development and Swedish Natural Science Research Council for generous financial support. Authors also thank Wallenbergs Stiftelse, University of Uppsala and Swedish Research Council (FRN) for funds toward the purchase of 500 MHz NMR spectrometer.

References

1. (a) Kole, R.; Altman, S. *Proc. Natl. Acad. Sci. U. S. A.* **1979**, *76*, 3795-3799; (b) Foster, A. C.; Symons, R. H. *Cell* **1987**, *49*, 211; (c) Uhlenbeck, O. C. *Nature* **1987**, *328*, 596.
2. (a) Buzayan, J. M.; Gerlach, W. L.; Bruening, G. *Nature* **1986**, *323*, 349, (b) Hampel, A.; Tritz, R. *Biochemistry* **1989**, *28*, 4929.
3. (a) Belinksy, M. G.; Britton, E.; Dinter-Gottlieb, G. *FASEB J.* **1993**, *7*, 130; (b) Sharmeen, L.; Kuo, M. Y. P.; Dinter-Gottlieb, G. *J. Virol.* **1988**, *62*, 685.
4. Saville, B. J.; Collins, R. A. *Cell* **1990**, *61*, 685.
5. Koizumi, M.; Ohtsuka, E. *Biochemistry*, **1991**, *30*, 5145.
6. (a) Fu, D.-J.; McLaughlin, L. W. *Proc. Natl. Acad. Sci. USA* **1992**, *89*, 3985; (b) Fu, D.-J.; McLaughlin, L. W. *Biochemistry* **1992**, *31*, 10941; (c) Pieken, W. A.; Olsen, D. B.; Benseler, F.; Aurup, H.; Eckstein, F. *Science* **1991**, *253*, 314; (d) Williams, D. M.; Pieken, W. A.; Eckstein, F. *Proc. Natl. Acad. Sci. USA* **1992**, *89*, 918; (e) Olsen, D. B.; Benseler, F.; Aurup, H.; Pieken, W. A.; Eckstein, F. *Biochemistry* **1991**, *30*, 9735.
7. (a) Heus, H. A.; Uhlenbeck, O. C.; Pardi, A. *Nucleic Acids Res.* **1990**, *18*, 1103; (b) Heus, H. A.; Pardi, A. *J. Mol. Biol.* **1991**, *217*, 113; (c) Pease, A. C.; Wemmer, D. E. *Biochemistry*, **1990**, *29*, 9039; (d) Odai, O.; Kodama, H.; Hiroaki, H.; Sakata, T.; Tanaka, T.; Uesugi, S. *Nucleic Acids Res.* **1990**, *18*, 5955.
8. (a) Kierzek, R. *Nucleic Acids Res.* **1992**, *20*, 5073; (b) Kierzek, R. *Nucleic Acids Res.* **1992**, *20*, 5079.
9. For a prelimiary communication of the self-cleavage of lariat RNA, see Agback, P.; Glemarec, C.; Yin, L.; Sandström, A.; Plavec, J.; Sund, C.; Yamakage, S.; Viswanadham, G.; Rousse, B.; Puri, N.; Chattopadhyaya, J. *Tetrahedron Lett.* **1993**, *34*, 3929.
10. Reese, C.B. *Tetrahedron* **1978**, *34*, 3143.
11. Zhou, X-X; Nyilas, A; Remaud, G; Chattopadhyaya, J. *Tetrahedron* **1987**, *43*, 4687.
12. Markiewicz, W *J.Chem. Res (S)* **1979**, 24.

13. Gioeli, C; Kwiatkowski, M.; Öberg, B.; Chattopadhyaya, J. *Tetrahedron Lett* **1981**, *22*, 1741.
14. Zhou, X-X; Remaud, G; Chattopadhyaya, J. *Tetrahedron* **1988**, *44*, 6471.
15. Sandström, A; Kwiatkowski, M.; Chattopadhyaya, J. *Acta Chem. Scand.* **1985**, *B39*, 273.
16. (a) Sund, C.; Földesi, A.; Yamakage, S-I.; Agback, P.; Chattopadhyaya, J. *Tetrahedron* **1991**, *47*, 6305; (b) Agback, P.; Glemarec, C.; Sund, C.; Chattopadhyaya, J. *Tetrahedron* **1992**, *48*, 6537.
17. Bannwarth, W; Trzeciak, A. *Helv. Chim. Acta* **1987**, *70*, 175-186.
18. Beaucage, S.L.; Iyer, R.P. *Tetrahedron* **1992**, *48*, 2223.
19. Sund, C.; Agback, P.; Chattopadhyaya, J. *Tetrahedron* **1993**, *49*, 649.
20. Gorenstein, D. G.; Findlay, J. B.; Momii, R. K.; Luxon, B. A.; Kar, D. *Biochemistry* **1976**, *15*, 3796.
21. Griesinger, C.; Otting, G.; Wuttrich, K.; Ernst, R. R. *J. Am. Chem. Soc.* **1988**, *110*, 7870.
22. Morris, G. A. *Magn. Reson. Chem.* **1986**, *24*, 371.
23. Bax, A.; Davies, D. G. *J. Magn. Reson.* **1985**, *63*, 207.
24. Derome, A.; Williamson, M. *J. Magn. Reson.* **1990**, *88*, 177.
25. Bax, A.; Griffey, R. H.; Hawkins, B. L. *J. Magn. Reson.* **1983**, *55*, 301.
26. de Leeuw, F. A. A. M.; Altona, C. *J. Chem. Soc. Perkin* II **1982**, *101*, 413.
27. Schmieder, P.; Ippel, J. H.; van den Elst, H.; van der Marel, G. A.; van Boom, J. H.; Altona, C.; Kessler, H. *Nucl. Acids Res.*. **1992**, *20*, 4747.
28. Altona, C. *Recl. Trav. Chim. Pays-Bas* **1982**, *101*, 413.
29. Lankhorst, P. P.; Haasnoot, C. A. G., Erkelens, C.; Altona, C. *J. Biomol. Struct. Dyn.* **1984**, *1*, 1387.
30. Lankhorst, P. P.; Haasnoot, C. A. G., Erkelens, C.; Westerink, H. P.; van der Marel, G. A.; van Boom, J. H. and Altona, C. *Nucl. Acids Res.* **1985**, *13*, 927.
31. (a) Davis, P. W.; Hall, K.; Cruz, P.; Tinoco, Jr. I.; Neilson, T. *Nucleic Acids Res.* **1986**, *14*, 1279; (b) Davis, P. W.; Adamiak, R. W., Tinoco, I. Jr. *Biopolymers* **1990**, *29*, 109.
32. Tran-Dinh, S., Taboury, J., Neumann, J.-M., Huynh-Dinh, T., Genissel, B., Langlois d'Estaintot, B., Igolen, J. *Biochemistry* **1984**, *23*, 1362.
33. Feigon, J.; Wang, A. H.-J.; van der Marel, G. A.; Van Boom, J. H.; Rich, A. *Nucl. Acids Res.* **1984**, *12*, 1243.
34. Wyatt, J. R.; Puglisi, J. D.; Tinoco, I. Jr *J. Mol. Biol.* **1990**, *214*, 455.
35. Campbell, I. D.; Dobson, C. M.; Ratcliffe, R. G.; Williams, R. J. P. *J. Magn. Reson.* **1978**, *29*, 397.
36. Neuhaus, D.; Williamson, M. in "The Nuclear Overhauser Effect in Structural and Conformational Analysis", **1989**, 143.
37. In a system in slow exchange between two forms A and B, the equilibrium is controlled by the foward and backward first-order rate constants k_a and k_b with $k_a/k_b = [B]/[A]$. On saturation of a resonance S of the B form, the steady-state intensity of the same resonance in the A form is given by: $fS^A \{S^B\} = S^{A'} - S^A/S^A = S^B/S^A * (k_a/(k_b + \rho S^A))$ where $S^{A'}$ is the magnetization of A upon saturation of B, S^A and S^B are the magnetizations at equilibrium, and ρS^A is the relaxation rate constant. The condition for chemical equilibrium implies: $k_a S^A = k_b S^B$ and $fS^A = k_a / (k_a + \rho S^A)$. It is assumed that the relaxation term ρ is temperature independent, then k_a is the only term which depends on temperature. A plot of $Ln(k_a/(k_a+\rho))$ against 1/T should give a straight line with the slope being the energy of activation E_a (from the Arrhenius equation: $k_a = Aexp[-E_a/RT]$).
38. $k_a/(k_a+\rho)$ for Na^+ salt at 288, 298, 303, 308, 313 and 318K is as follows: 0.03, 0.10, 0.20, 0.39, 0.79 and 1.70 s^{-1}. 38. $k_a/(k_a+\rho)$) for Et_3N salt at 288, 295, 298, 303, 308, 313 and 318K is as follows: 0.04, 0.08, 0.12; 0.16, 0.44, 0.62 and 1.70 s^{-1}.
39. Low energy conformers of the two hexameric and the heptameric lariat structures were found after an extensive search of conformational space using the Monte Carlo option of the Macromodel program package. 10000 conformers were generated for each of the three lariats. The structures were then subjected to constrained energy minimizations and constrained molecular dynamics simulations using the SANDER module of the AMBER 4.0 program package (see ref. 44) with the supplied all atom force field, parm91. The constraints (β, γ, ε, ν_0, and ν_2, and χ) were derived (see refs. 29 and 45) from NMR ^1H-^1H, ^1H-^{31}P, and ^{13}C-^{31}P coupling constants and NOESY and ROESY intensities. Additional constraints, in the form of improper torsions, were required to maintain the correct chirality of the carbon atoms of the sugar residues. Three stages of constrained conjugate gradient minimizations were used (i; 200 steps. ii; Until rms gradient < 0.25 kcal.mol^{-1}.Å^{-1}. iii; Until rms gradient < 0.001 kcal.mol^{-1}.Å^{-1}) and only the low energy conformers were passed on to the next stage of minimization. After the third and final stage of minimization 21 conformers of the A-form hexamer, 32 conformers of the B-form hexamer, and 27 conformers of the heptamer remained. Each of these structures were taken as initial conformers for 25 ps of MD simulations at 400 K. "Snapshots" were taken every 0.5 ps during the final 10 ps of each MD simulation and these structures were energy minimized. Thus 420 conformers of

A-form hexamer, 640 B-form hexamer, and 540 heptamer conformers were obtained. All minimizations and molecular dynamics so far were done in vacuum with a distance dependent dielectric ($\varepsilon = 4r_{ij}$) and infinite cutoffs for nonbonded interactions. During all MD simulations, both in vacuum and with water, the shake algorithm (see ref. 46) was used for bond lengths involving hydrogens.

40. The *lowest energy conformer* from the *in vacuo* minimization/dynamics procedure of the A-, and B-form hexamer and the heptamer were used as initial conformations for the 226 ps MD simulations in water using periodic boundary conditions. The SANDER module of the AMBER 4.0 program (see ref. 44) was used with some alterations of the supplied all atom force field, parm91. 6-12 and 10-12 parameters for interactions between water hydrogens (HW) and water oxygens (OW) are originally set to zero. In addition we set the 10-12 parameters for interactions between any atom and OW as well as any atom and HW to zero, the 6-12 parameters for hydrogen bonding hydrogens were also set to zero (see ref. 47). Sodium ions, six for hexamers and seven for heptamer, were added to the initial conformers by placing them at the O=P-O$^-$ bisector with a 5 Å distance to the phosphorous atom. 64 Cubes of 216 TIP3P water molecules (see ref. 48) were added followed by the removal of water molecules being either too close (3.0 Å for oxygen, 2.2 Å for hydrogens) or too distant (7.1, 9.0, and 10.0 Å for A-form hexamer in X-, Y-, and Z-directions respectively, 9.0, 9.0, and 9.0 Å for B-form hexamer, and 5.5, 9.0, and 10.0 Å for heptamer) from the solute. The two hexamer structures were each solvated by 1130 water molecules and the heptamer was solvated by 1156 water molecules. Two energy minimizations were performed on the three solvated structures; i) 500 steps of steepest descent where the solute was held fixed, ii) 500 steps (100 steps SD and 400 steps conjugate gradient) with NMR-derived torsional constraints turned on (see Table 6). The energy minimized structures were then subjected to 226 ps of MD (0-2 ps at 300 K where the water box volume was held constant, 2-4 ps at 100 K, 4-6 ps gradual increase of temperature to 284 K, and 6-226 ps at 284 K). The temperature was held at the desired temperature using the Berendsen algorithm (see ref. 49) with separate couplings to the heat bath for solute (τ_{tp}= 0.1 ps) and solvent (τ_{ts} = 0.2 ps). During 54 ps (2-56 ps) the pressure of the system was coupled to a pressure bath (see ref. 49) of 1 atm (τ_p = 0.1 ps for 2-6 ps, τ_p = 0.2 ps for 6-56 ps). The volume obtained at 56 ps was then used for the constant volume simulations (56-226 ps). The three sides of the water box each decreased by approximately 5 % (~14 % decrease in volume) during the 54 ps of constant pressure MD. The NMR-derived torsional constraints were used during the first 96 ps, they were gradually turned off over a 10 ps period (96-106 ps) and during the final 120 ps (106-226 ps) the constraints were not used at all. During the entire MD simulations including water the cutoff distance for nonbonded interactions was set to 9.5 Å and the nonbonded list was updated every 25 fs.

41. Taira, K.; Uebayasi, M.; Furukawa, K *Nucleic Acids Res.* **1989**, *17*, 3699.
42. Holbrook, S. R.; Cheong, C.; Tinoco, I.; Kim, S.-H. Nature, **1991**, *353*, 579.
43. Chowrira, B. M.; Berzal-Herranz, A.; Burke, J. *Nature*, **1991**, *354*, 320.
44. Pearlman, D. A.; Case, D. A.; Caldwell, J. C.; Seibel, G. L.; Singh, U. C.; Weiner, P.; Kollman, P. A. AMBER 4.0, University of California, San Fransisco, **1991**.
45. Haasnoot, C. A. G.; de Leeuw, F. A. A. M.; de Leeuw, H. P. M.; Altona, C. *Recl. Trav. Chim. Pays-Bas*, **1979**, *98*, 576.
46. Ryckaert, J. P. *Mol. Phys.*, **1985**, *55*, 549.
47. Dang, L. X.; Kollman, P. A. *J. Am. Chem. Soc.*, **1990**, *112*, 503.
48. Jorgensen, W. L.; Chandrasekhar, J.; Madura, J. D.; Impey, R. W.; Klein, M. L. *J. Chem. Phys.*, **1983**, *79*, 926.
49. Berendsen, H. J. C.; Postma, J. P. M.; van Gunsteren, W. F.; DiNola, A.; Haak, J. R. *J. Chem. Phys.*, **1984**, *81*, 3684.
50. Agback, P.; Sandström, A.; Yamakage, S.; Sund, C.; Glemarec, C.; Chattopadhyaya, J. *J. Biochem. Biophys. Methods* , **1993**, *27*, 229.

(*Received in UK* 8 *October* 1993; *revised* 2 *November* 1993; *accepted* 5 *November* 1993)